Journal of Wind Engineering & Industrial Aerodynamics 236 (2023) 105360

Contents lists available at ScienceDirect

Journal of Wind Engineering & Industrial Aerodynamics

journal homepage: www.elsevier.com/locate/jweia

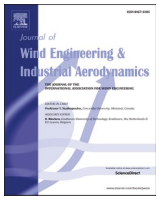

Review of wind loading on roof to wall connections in low-rise light wood-frame residential buildings

Kehinde J. Alawode [a,*], Krishna Sai Vutukuru [b], Amal Elawady [a,c], Arindam Gan Chowdhury [a,c]

[a] Department of Civil and Environmental Engineering, Florida International University, Miami, FL, USA
[b] Thornton Tomasetti, Fort Lauderdale, FL, USA
[c] Extreme Events Institute of International Hurricane Research Center, Florida International University, Miami, FL, USA

ARTICLE INFO

Keywords:
Roof to wall connections
Wind loads
Low-rise wood-frame buildings
Hurricane

ABSTRACT

Several post-hurricane studies have indicated the prevalence of roof damage in low-rise wood-frame buildings. One of the major reasons for this includes failure of roof-to-wall connections (RTWCs). This has led to a lot of research on RTWCs in a bid to understand the reasons for the failures, the capacities of the RTWCs and development of better RTWCs especially in hurricane prone regions. This study reviews the research works to date on factors affecting wind loads on RTWCs. It explores the experimental tests on RTWCs in roofing structures and component tests of single RTWCs. Numerical and analytical modeling of RTWCs as part of a roof system or as single connections are all reviewed. Finally, recommendations for future research works to bridge current knowledge gaps are made.

1. Introduction

Roof-to-wall connections (RTWCs) in low-rise light wood frame residential buildings are the means by which the roof structure (i.e., trusses) is connected to walls. Fig. 1 shows the main components of a typical roof system of low-rise residential buildings which includes roof truss, battens, roof sheathing, wall plates, ceilings and RTWCs. The roof truss comprise of top chords, bottom chords and webs/struts which give the roof its structural form. The battens run across the trusses and provide a base for the roof sheathing. The roof sheathing is a wooden board that serves as a base for roof tiles in many low-rise buildings. The essential structural function of the RTWCs is to provide a load path for uplift roof loads to the supporting walls and the transfer of lateral loads (due to wind, rain, hail, or earthquake) through the walls to the building's foundations (Shanmugam et al., 2011). RTWCs currently being used include toe-nailed connections (which consist of nails only), metal straps, hurricane straps, fiber-reinforced polymers (FRP) and triple grip connectors, among others. Schematics of some RTWCs are shown in Fig. 2. The selection of an appropriate RTWC usually depends on the type of construction and the magnitude of the environmental loads acting on the connectors. The focus of this paper would be on RTWCs as a part of the roofing system to provide the load path.

Approximately 90% of residential roofs in the USA are wood framed (Ellingwood et al., 2004). In strong winds, the uplift loads are only partially offset by the roof dead loads (Reed et al., 1997a), making the role of RTWCs important in structures. RTWCs have been identified as the weak link in many low-rise structures during extreme wind events. Shanmugam et al. (2009) attributed the failure of residential roofs during hurricanes to the poor performance of RTWCs. Also, post-hurricane surveys have identified loss of roof as the most serious structural damage (FEMA, 2005; Pinelli et al., 2018; Prevatt et al., 2021). Municipalities with high wind hazards such as the State of Florida have therefore issued stringent building code requirements to help mitigate damage to buildings during extreme wind events.

In studies on RTWCs (e.g. Shanmugam et al., 2009; Ahmed et al., 2011; Edmonson et al., 2012), experimental tests focused on determining the uplift capacity of joints based on the loading requirements in standards such as the ASTM D1761(ASTM 2020). Conner et al. (1987) and Reed et al. (1997a) applied loads calculated from wind loading standards such as the ANSI A58.1 (ANSI 1982) and ASCE 7–93 (ASCE 7-93, 1993), while Canino et al. (2011) and Chowdhury et al. (2013) used wind tunnel aerodynamic loads based on factors affecting the uplift and lateral loads in RTWCs, i.e., the enclosure classification (closed or partially enclosed), rain effects and terrain conditions.

This paper presents a state-of-the-art review of previous research works as it relates to wind loads on RTWCs in low-rise light wood-frame residential buildings, presenting knowledge gaps and areas for further

* Corresponding author.
E-mail address: kalaw003@fiu.edu (K.J. Alawode).

https://doi.org/10.1016/j.jweia.2023.105360
Received 13 October 2022; Received in revised form 7 February 2023; Accepted 19 February 2023

Notations

$\overline{C_{p_i}}$	Mean internal pressure coefficient
$\overline{C_{p_w}}$	windward external pressure coefficients
$\overline{C_{p_L}}$	leeward external pressure coefficients
p_o	reference atmospheric pressure
n	polytropic exponent
$\ddot{C}_{p_i}$	second derivative of internal pressure
$\dot{C}_{pi}$	first derivative of internal pressure
q	dynamic pressure
A	small opening area
C_{pe}	external pressure
p	pressure
C_{pi}	internal pressure
a_s	speed of sound
K_A	bulk modulus of air
p_o	atmospheric pressure (static)
ρ	air density
V_o	internal volume
q	dynamic pressure
K_B	bulk modulus of building
S*	leakage area to volume parameter

research. Section 2 and Section 3 of the paper discuss external and internal wind pressures, respectively, as major factors in determining wind loads on RTWCs. Section 4 discusses numerical, experimental, and analytical methods used in the study of RTWCs. Section 5 discusses load sharing in RTWCs, and Section 6 discusses current design recommendations. Section 7 provides key conclusions on the current knowledge of RTWCs and provides directions for further studies.

2. External pressures and their effects on RTWCs

External pressures due to wind cause lateral and uplift loads on roofs (Ahmad and Kumar, 2002). During extreme wind events, high uplift forces are exerted on roofs (i.e., entire roof system) due in part to high suctions caused by vortices induced by fluid-structure interaction (Feng et al., 2020). RTWCs are the only intermediary between the roof structure and the walls and must be capable of transferring those forces to the foundation, so that roof or other component-level failures do not occur.

He et al. (2017) summarized the factors affecting external pressures in low-rise buildings. These factors are discussed in the following sub-sections, while Table 1 summarizes the implication of these factors. The following sections discuss various parameters that affect the loads on the RTWCs in a typical building.

2.1. Upstream terrain

Most building codes classify building exposure in flat terrain as open country, suburban and urban. The distinction is based on the respective features of the atmospheric boundary layer (ABL) (Stathopoulos, 1984). Case and Isyumov (1998) noted a 15%–25% reduction in wind loads on isolated buildings with suburban exposure with respect to buildings with open exposure. Other studies (Stathopoulos et al., 1979; Ho et al., 1991; Meecham et al., 1991; Gerhardt and Kramer, 1992; Lin et al., 1995; Case and Isyumov, 1998; Stathopoulos, 2003; Pierre et al., 2005; Gavanski et al., 2013) confirmed such differences. Fig. 3 shows an example of the effect of the terrain on the peak uplift coefficient for different eave heights (Pierre et al., 2005). However, no study has specifically addressed the dependence on terrain exposure of forces on RTWCs. Such a study could be useful for retrofitting buildings in suburban areas that are gradually becoming more urbanized.

2.2. Roof shape

The most common type of roofs in low-rise buildings are gable and hip roofs, although gable roofs have received the most attention in aerodynamic load studies (Meecham et al., 1991). Post-disaster reports which indicated the resilience of hip roofs compared to gable roofs led Meecham et al. (1991) to undertake a wind tunnel study on 18.4° pitched roofs, comparing the pressures and uplift forces in the two roof types. Their study indicated that in both open country and suburban terrains, trusses of hip roofs are subjected to about 50% weaker local peak negative pressures as well as weaker uplift forces in comparison to gable roofs. The roof uplift forces create reaction forces in the RTWCs (Meecham et al., 1991). Xu and Reardon (1998) compared the wind pressure coefficients on hip roofs with pressure coefficients on gable roofs as determined by Holmes (1981) for buildings with similar roof pitches. From that study, Xu and Reardon (1998) concluded that gable roofs experience roof suctions stronger than those acting on hip roofs. Meecham et al. (1991) reported a similar conclusion (Fig. 4) but noted that the difference between the overall (i.e., entire roof) instantaneous uplift in hip and gable roofs is negligible.

Stathopoulos and Mohammadian (1986) showed that monoslope roofs experience higher wind-induced loads than flat or gable roofs. In multi-span gable roofs, Stathopoulos and Saathoff (1991) noted a higher magnitude of negative pressure coefficients than that of single-span

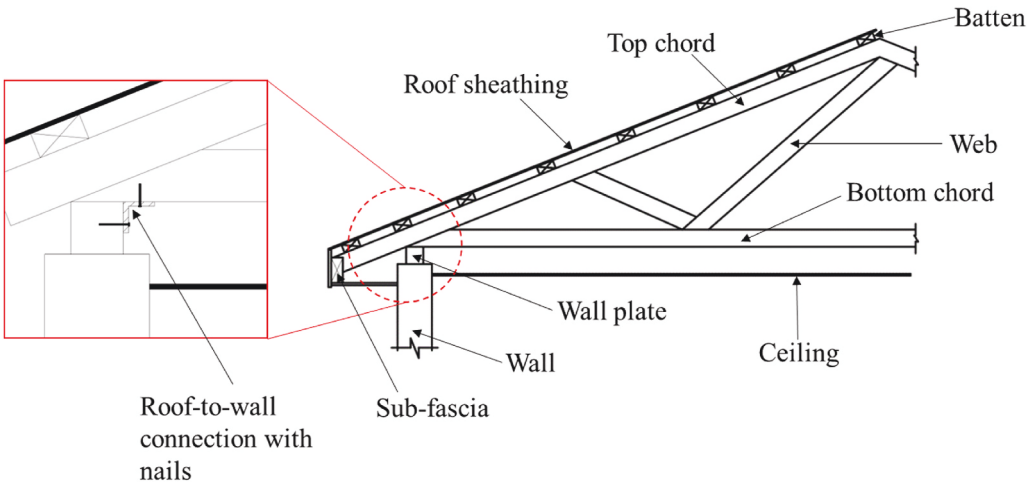

Fig. 1. Schematic of a typical roof system of low-rise residential buildings.

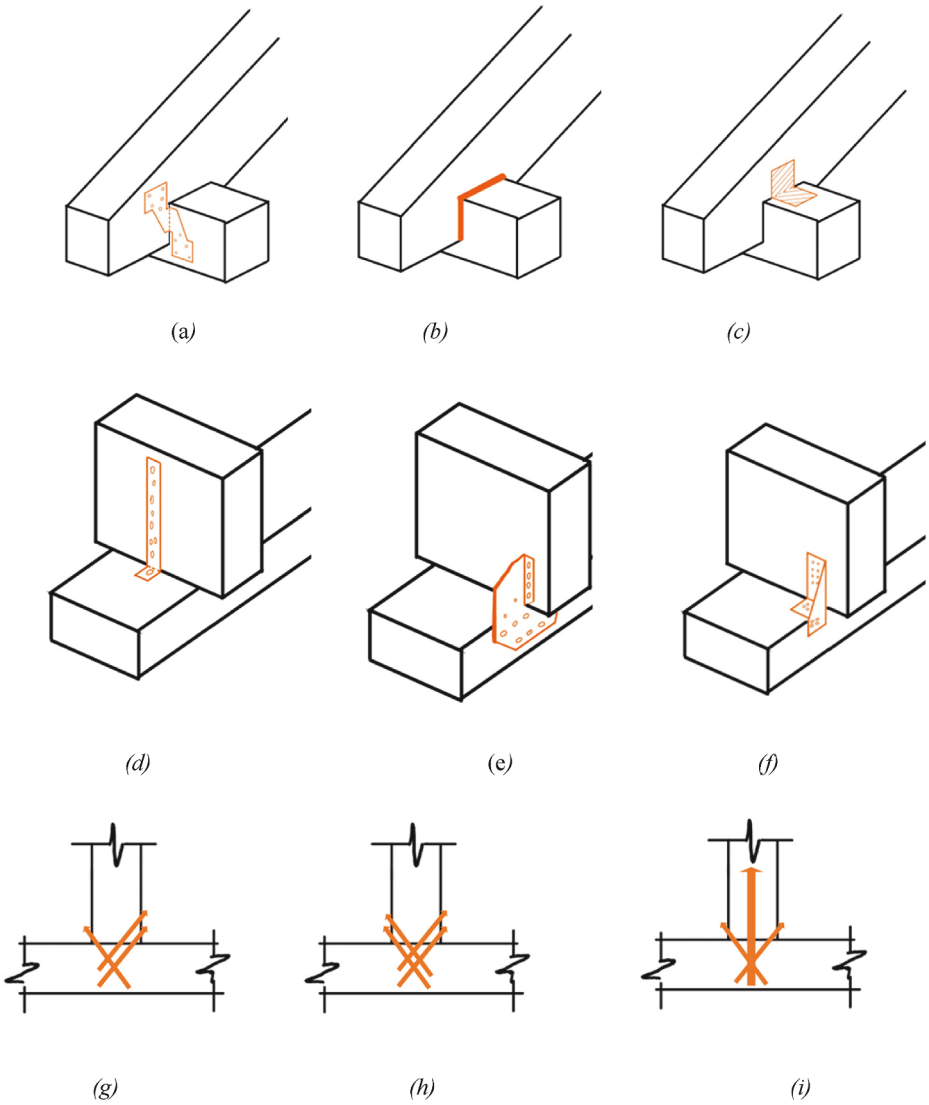

Fig. 2. Schematic of Several RTWCs (a) Hurricane clip; (b) Epoxy/Adhesive; (c) Fiber reinforced polymer (FRP) connector; (d) Hurricane strap; (e) Flat plate connector; (f) Triple grip connector; (g) 3-16d toenail connection; (h) 2-16d + 3-16d toenail connection; (i) 3-16d toenail and lag bolt.

roofs, especially in the troughs and roof corners. Regarding curved roofs, Franchini et al. (2005) noted that for oblique wind directions high suctions occur at the corners irrespective of curvature.

To summarize, all above-mentioned studies indicated the importance of roof shapes in estimating wind loads on roofs; RTWCs in hip roofs are subjected to lesser uplift forces than gable roofs, RTWCs in flat and gable roofs experience lesser wind forces in comparison with mono-sloped roofs, and RTWCs in single span roofs have lesser wind forces that those in multi-span roofs.

However, as distinct from gable, hip, or flat roofs of buildings with a rectangular or square plan, roofs that are a combination of both gable and hip roofs as well as having multiple spans have received very little attention (Shao et al., 2018), even though roof shapes determine the wind separation mechanism on the roof, making it an important factor affecting the magnitude of wind-induced uplift forces on roofs (Stathopoulos, 2003). A study that compiles an aerodynamic database of pressure coefficients on roofs of different shapes would be a good addition to currently available data on conventional roofs.

2.3. Roof pitch

Holmes (1981) compared wind pressure coefficients of gable roofs with pitches of 15°, 20° and 30°. Similarly, Gavanski et al. (2013) and, Xu and Reardon (1998) compared almost similar pitches of hip roofs, with Gavanski et al. (2013) adding 36° and 45° pitch angles. The results by Xu and Reardon (1998) indicate that the roof suction increases with increasing pitch angle, with the 30° pitch roof having the highest suction. Also, a noteworthy observation was that both hip and gable roofs had similar suction at roof pitch angles of 30°. In multi-span gabled roofs, Stathopoulos and Saathoff (1991) observed larger magnitude of negative peak pressures in the 12:12 (45°) roofs in comparison to the 4:12 (18.43°) roofs. Mean pressure coefficients on the hip roofs tested by Gavanski et al. (2013) are shown in Fig. 5 which indicates higher suction Cp with increasing roof pitch at a wind direction perpendicular to the roof edge.

These studies indicated that RTWCs would experience higher uplift wind loads with increasing roof pitch up to 27°. ASCE 7–22 reflects this in its provisions for roof wind loads. The influence of roof pitch on RTWC wind loads has not been studied. A quantifiable factor for increased or reduced RTWC load depending on roof pitch can be beneficial for design engineers.

Table 1
Implication of external pressure parameters on RTWCs.

Parameter	General conclusion/ inference of effect on RTWC	Reference
Upstream Terrain	Open terrain indicates higher wind loads on RTWC compared to sub-urban/ urban terrain	Ho et al. (1991); Meecham et al. (1991) Case and Isyumov (1998); Gavanski et al. (2013)
Roof Pitch	It can be inferred that higher roof pitches (up to 27°) translate to higher uplift loads on RTWCs especially those at the edges	Stathopoulos and Saathoff (1991); Xu and Reardon (1998); Holmes (1981); Gavanski et al. (2013); ASCE 7-22
Roof shape	RTWCs in hip roofs are subjected to lesser uplift forces than gable roofs across both open and sub-urban terrain	Stathopoulos and Mohammadian (1986); Meecham et al. (1991); Stathopoulos and Saathoff (1991); Xu and Reardon (1998); Franchini et al. (2005);
Building geometry	For a 30° roof pitch, aspect ratios have a higher effect on the loads on RTWCs than the overhang ratios.	Ahmad and Kumar (2002)
Wind direction	Oblique wind angles present the worst wind loads for RTWCs and as the loads are higher at roof corners, the RTWCs at corners are most vulnerable.	Kind (1988); Lin et al. (1995); Xu and Reardon (1998); Shao et al. (2018); Shao et al. (2019)
Presence of a canopy and parapet	The presence of parapets and cantilevered canopies, especially porous ones reduce roof uplifts, translating into lesser loads on RTWCs.	Lythe and Surry (1983); Baskaran and Stathopoulos (1988); Kind (1988); Pindado and Meseguer (2003); Franchini et al. (2005); Blessing et al. (2009); Azzi et al. (2020)
Presence of surrounding buildings	The presence of surrounding buildings reduces the wind loads due to shielding effects but increases fluctuating pressures. This could translate to lower wind loads but high chances of fatigue in RTWCs.	Ho et al. (1991); Case and Isyumov (1998); Wu and Kopp (2018)

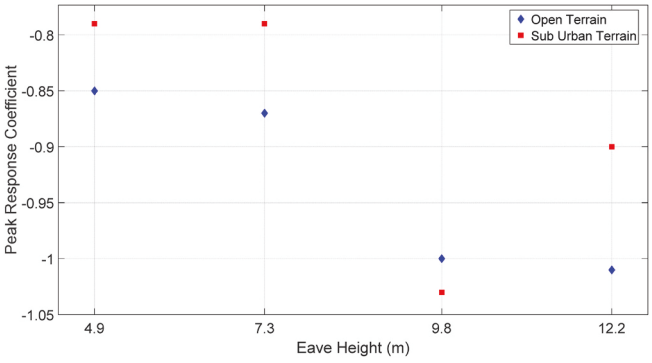

Fig. 3. Peak response dependence on eave height (St. Pierre et al., 2005).

2.4. Building geometry (plan shape, height, overhangs, aspect ratios)

Ahmad and Kumar (2002) observed an increase in the peak suction pressure coefficient (C_{pmin}) and root mean square of pressure coefficient (C_{prms}) on roofs with increasing aspect ratio (eave height/constant base width of 140 mm) of 0.4, 0.5 and 0.6, in their study on hip roofs with 30° pitch. In their study, the variation of overhang ratio (eave height/-overhang) of 0.17, 0.26 and 0.38, in hip roofs were shown to have moderate effects on roof pressures. Minimum peak pressure coefficients C_{pmin} have been found to occur at the edge corner for the overhang ratio of 0.26. Edge corners and hip ridges are locations of higher wind loads, consequently, the RTWCs at the edge corners would be subjected to higher wind loads.

The study by Shao et al. (2018) concludes that there is very little difference in the wind pressures on T and L-shaped plan roofs. In comparison with rectangular-shaped plan roofs, the L and T-shaped plan roofs have higher suction pressures induced by oblique winds. Wind tunnel tests by Stathopoulos and Luchian (1990) indicated that the lower section of a multilevel flat roof experiences higher positive wind pressures in comparison with flat roofs of uniform height. Also, the higher flat roofs in the multi-level flat roof experience stronger suction than the lower flat roofs. This is due to the increase in wind speed with height and the values are similar to simple flat roofs at the same height. In monoslope roofs, Stathopoulos and Mohammadian (1986) observed an increase in suction pressures on roof corners with increasing heights.

This indicates that RTWCs in rectangular plan shaped buildings have lesser wind pressures than those in T and L plan shaped buildings, RTWCs in uniform height roofs have lesser wind pressures than stepped buildings with flat roofs, and RTWCs in low height monoslope roofs are subjected to lesser wind pressures than those of higher heights. While this can be interpreted from existing research works, a quantifiable value of this difference is unknown and this gap in knowledge can be filled by future works specifically focusing on RTWCs in different shapes of buildings.

2.5. Wind direction

Wind direction is a factor affecting the external pressures of roofs that cannot be controlled by the design engineer. Hence, the practice is usually the use of the worst/peak C_p envelope for design purposes.

Flat roofs are susceptible to conical vortices for wind directions varying from 15° to 75° depending on the geometry and roof shape of the building (Lin et al., 1995). The 45° wind direction has been identified as the wind attack angle that causes the peak suction at roof corners in flat, hip and gable roof types (Kind, 1988; Shao et al., 2018; Xu and Reardon, 1998). This is due to the formation of conical vortices which create high suctions at the edges and the ridge of roofs. A similar observation about oblique winds was made for non-rectangular plan hip-roofs by Shao et al. (2019). Ahmad and Kumar (2002) observed 120° wind direction as critical for all hip roofs they tested in their study. Oblique winds would therefore present the highest loads on RTWCs, especially those at or near roof corners.

2.6. Presence of canopy and parapet

Many researchers (including; Lythe and Surry, 1983; Kind, 1988; Baskaran and Stathopoulos, 1988; Pindado and Meseguer, 2003; Franchini et al., 2005; Blessing et al., 2009; Azzi et al., 2020) have shown that the presence of parapets on roofs helps to reduce suctions at the roof edges. The area affected by high suctions in flat roofs is usually a small portion of the windward edge as the absolute C_p decreases as the inverse of the square root of the ratio of distance to the windward roof corner and roof height (Lin et al., 1995).

Investigations by Baskaran and Stathopoulos (1988), Kind (1988) and, Lythe and Surry (1983) on flat roof models concluded that the magnitude of suctions at the edge of the roof decreases with increasing parapet heights. The reason for the decreasing suction is that higher parapet heights cause the flow to reattach further down the roof length. In addition, parapets decrease the frequencies of fluctuating pressures (Baskaran and Stathopoulos, 1988). It is noteworthy that Lythe and Surry (1983) found low-height parapets on low-rise buildings to cause higher suction pressures at roof corners while Baskaran and Stathopoulos (1988) concluded that having parapets on one side of the roof causes higher suctions.

Perforated parapets have also been a subject of research as a means of reducing wind-induced uplifts on roof corners. Baskaran and

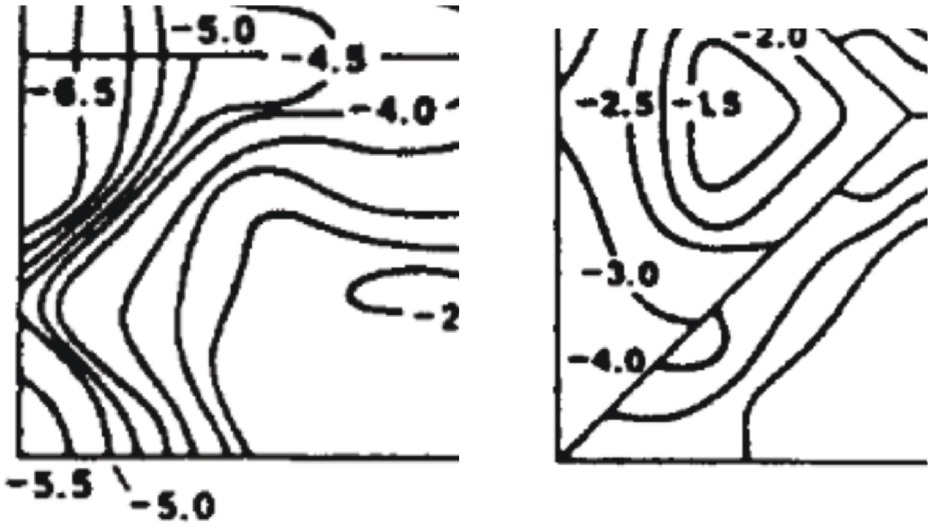

Fig. 4. Worst peak corner negative pressure coefficient (Reprinted from Meecham et al. (1991).

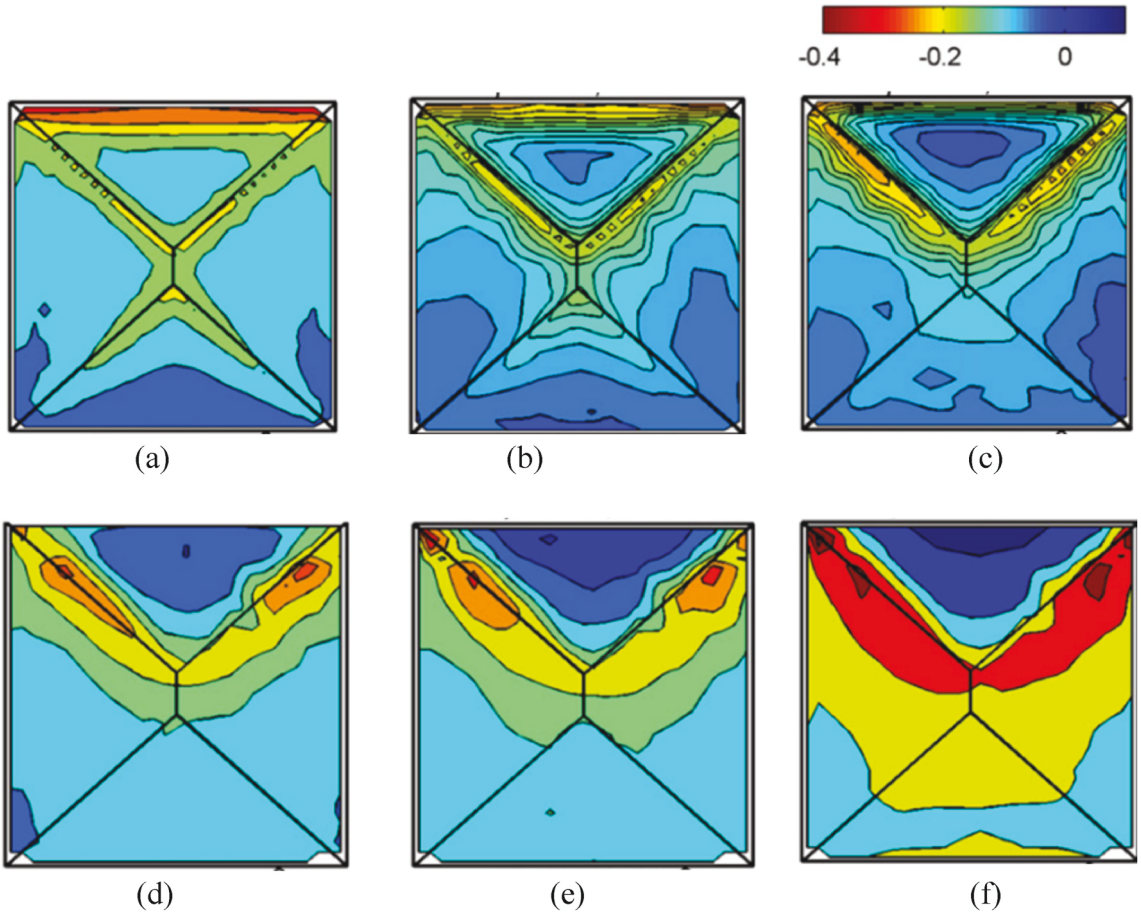

Fig. 5. Mean pressure coefficient on hip roofs of (a)18.43°, (b)22.6°, (c)27°, (d)30.2°, (e)36° and (f)45° pitch (reprinted from Gavanski et al., 2013).

Stathopoulos (1988) compared suctions in the presence of low parapets with slots, parapets with no slots, and in the absence of parapets. They concluded that slots can help to reduce high suctions. Pindado and Meseguer (2003) and Surry and Lin (1995) reached the same conclusion. A recent study by Azzi et al. (2020) indicates that discontinuous perforated parapets installed at roof corners effectively reduce suctions by 40% (area averaged peak pressure coefficients).

Canopies have also been studied, although most focused on the

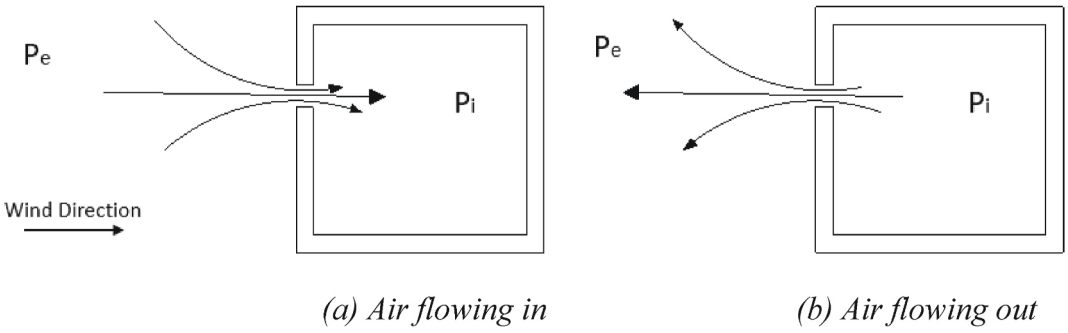

Fig. 6. Air Flow through an opening.

Table 2
List of the development of the internal pressure theory.

Author and Year	Major Contribution	Derived Expression/Conclusion	References that confirmed the equations or extended the application area
Irminger and Nokkentved (1930)	Flow Rate	$Q_i = \pm A_j V_j = \pm k A_j \sqrt{\frac{2\lvert p_j - p_i \rvert}{\rho}}$	
Liu (1975)	Continuity	$\overline{C_{p_i}} = \frac{\overline{p_i} - p_o}{q} = \frac{\overline{C_{p_w}}}{1 + \left(\frac{A_L}{A_W}\right)^2} + \frac{\overline{C_{p_L}}}{1 + \left(\frac{A_L}{A_W}\right)^2}$	
Holmes (1979)	- Buildings with openings behave like a Helmholtz resonator - Correct volume scaling for wind tunnel tests - Non-dimensional form of the governing equation	$C_{pe} = \frac{\rho l_e V_o}{A n p_o} \ddot{C_{p_i}} + \frac{\rho V_o^2 q}{2k^2 n^2 A^2 p_0^2} \dot{C_{pi}} \lvert \dot{C_{pi}} \rvert + C_{pi}$ n = 1.2 k = 0.6 and 0.15	Fahrtash and Liu (1990) and Liu and Rhee (1986) n = 1.23
Liu and Saathoff (1981)	- Rigorous derivation using Bernoulli's Equations	$C_{pe} = \frac{\rho l_e V_o}{k A n p_o} \ddot{C_{p_i}} + \frac{\rho V_o^2 q}{2k^2 n^2 A^2 p_0^2} \dot{C_{pi}} \lvert \dot{C_{pi}} \rvert + C_{pi}$ n = 1.4, k = 0.88	Liu and Rhee (1986), Saathoff and Liu (1983) and Stathopoulos and Luchian (1989) n = 1.4, k = 0.88
Vickery (1986)	- Including the role of building envelope flexibility in internal pressures	For uniform leakage and For buildings with an opening equal to or greater than about twice background leakage (dominant opening) $C_{pe} = \frac{1}{\omega_o^2} \ddot{C_{p_i}} + \frac{\beta^2}{\omega_o^2} \dot{C_{pi}} \lvert \dot{C_{pi}} \rvert + C_{pi}$ Where; $p = C_p^{1/2} \rho \overline{V^2}$ $\beta = \frac{\sqrt{C_L}}{2} \frac{\overline{V}}{a_s} \frac{V_0^{1/2}}{\left[V_0\left(1 + K_{A/K_B}\right)\right]^{1/4}}$ $\omega_0 = \frac{a_s a^{1/4}}{\left[V_o\left(1 + K_{A/K_B}\right)^2\right]^{1/4}}$	Pearce and Sykes (1999) and Estephan et al. (2021)
Saathoff and Liu (1983)	- multiple rooms and partitions	A series of simultaneous equations need to be solved to observe the internal pressure coefficient for a multi-room system E.g., for 2 room building with one windward opening the equations are 1 $L_e \dot{V}_{j1} = \frac{P_e - P_1}{\rho} - \frac{1}{2} V_{j1} \lvert V_{j1} \rvert$. 2 $L_e \dot{V}_{j2} = \frac{P_1 - P_2}{\rho} - \frac{1}{2} V_{j2} \lvert V_{j2} \rvert$. 3 $\dot{p_1} = \frac{n p_a}{V_o} (A_1 V_{j1} - A_2 V_{j2})$. 4 $\dot{p_2} = \frac{n p_a}{V_o} A_2 V_{j2}$.	
Estephan et al. (2021)	- attenuation of external pressure close to the leakage area in nominally sealed buildings	$C_{pe} * (-14 S^{*2} + 20 S^* + 0.17) = \frac{\rho V_o^2 q}{2k^2 n^2 A^2 p_0^2} \dot{C_{pi}} \lvert \dot{C_{pi}} \rvert + C_{pi}$	

pressure coefficients on the canopies and not the entire roof under different configurations (i.e. Zisis and Stathopoulos, 2010; Zisis et al., 2017). Canopies that are at the same height as the roof or closer to the roof edge reduce net pressure coefficients on the roof (Zisis and Stathopoulos, 2010) as the separation zones move from the roof edge to the edge of the canopy. The results of the study by Pindado and Meseguer (2003) on flat roofs indicated that small horizontal parapets (canopies) are more effective than vertical parapets in reducing roof wind loads. Franchini et al. (2005) similarly concluded that small horizontal parapets (canopies) effectively reduce wind loads on curved roofs. In both Pindado and Meseguer (2003) and Franchini et al. (2005), the horizontal parapets were above the roof height. A study that focuses primarily on

the effect of canopies and parapets on the wind loads on RTWCs can further guide RTWC selection, especially at roof positions where the canopy or parapet is attached.

2.7. Presence of surrounding building

Prior to 1991, only a few studies (e.g., Hussain and Lee, 1980; Vickery, 1976; Walker and Roy, 1985) considered the effect of surrounding buildings on the external pressures on low-rise buildings. Ho et al. (1991) considered a building in a typical industrial area in North America and an isolated building and showed that the isolated building experienced higher wind loads than the building located in a city (or urban center). However, while mean wind loads were lower, fluctuating wind loads on roofs were higher for buildings in cities. A similar result was obtained by Case and Isyumov (1998). A study by Surry and Lin (1995) concluded that peak, mean and rms suctions on roofs were reduced by the presence of surrounding buildings.

Wind pressure fluctuations can have significant influence on fatigue loads in RTWCs (Vickery and Bloxham, 1992). An understanding of this connection can guide engineers in the selection of an appropriate RTWC. Chang and Meroney (2003) combined both experimental and numerical tests to study the effects of surrounding buildings and, like Surry and Lin (1995), noted a reduction in peak, mean and rms C_p's. They noted that the shielding effect was dependent on the ratio of distance between buildings and building height, and that shielding effects were higher in urban than in open country settings. However, there are no specific studies that have focused on the impact of surrounding buildings on RTWC loads.

3. Internal pressures and RTWCs

The crucial role of the internal pressures in determining the net wind loads on the building envelope (external walls and roofs) is now well recognized. The relative uniformity and small magnitude of internal pressures, unlike external pressures, in a nominally sealed building envelope (Ginger, 2000; Stathopoulos et al., 1979; Oh et al., 2007; Alawode et al., 2023) initially resulted in less focus and fewer studies on the internal pressures in buildings, in comparison to external pressures. However, an opening in the building envelope – produced either intentionally (e.g., by doors left open) or accidently (e.g., windows or doors broken by flying debris or small cracks of the envelope) results in high internal pressures, sometimes higher than external pressure fluctuations in situations of Helmholtz resonance, and could easily lead to increased roof suction and damage (Conner et al., 1987; Guha et al., 2011; Yeatts and Mehta, 1993). Experimental studies by Chowdhury et al. (2013) have shown that a case of the dominant opening could result in an approximately 5.5 times increase in net wind loads. This scenario is the governing design criterion as it is the worst possible case that could result from a wall and/or roof uplift failure (Holmes, 1979). To better understand the influence of internal pressures in cases of buildings with openings, it is useful to understand the theory behind it.

3.1. Theory

In studying internal pressures in low-rise buildings with openings, Holmes (1979) considered the building as a Helmholtz resonator. Helmholtz resonance is a concept used in acoustics. With a building idealized as a box (resonator) with an opening, a slug of air is pushed through the opening (defects in walls, doors or windows) into the building as depicted in Fig. 6a. Assuming the pre-existing air inside the building acts as a spring, this new slug of air powered by the external pressure (Pe) compresses this spring (i.e., internal air) until the pressure inside the building (Pi) becomes higher than Pe. At this point, the spring pushes back leading to an outward movement of the slug of air (such as in Fig. 6b) until Pe becomes greater than Pi. This back-and-forth movement (vibration) of the slug of air continues as Pi increases and decreases. Resonance occurs when the vibration matches the fundamental frequency of the box (which depends on opening size, the flexibility of the box, the presence of partitions, secondary openings, and leakages), resulting in a large fluctuation in Pi.

An expression describing the motion of the slug of air was derived by Holmes as a second-order, non-linear, ordinary differential equation that could predict the general behavior of internal pressure, its maximum value and time of occurrence. However, this expression is only applicable to small pressure variations (Stathopoulos and Luchian, 1989). Liu and Saathoff (1981) derived a similar expression using an approach based on Bernoulli's equation. This approach is considered to be more rigorous (Saathoff and Liu, 1983; Harris, 1990) and the expression applies to any pressure variation (Stathopoulos and Luchian, 1989). The other difference between Liu and Saathoff (1981) and Holmes (1979) is the presence of a 'k' factor (Contraction Coefficient) in the first term of the equation by Liu and Saathoff (1981) (Stathopoulos and Luchian, 1989), see Table 2. These two equations have been the basis of most of the research works on internal pressure in buildings. Experimental studies by Liu and Rhee (1986) showed that the Liu and Saathoff (1981) equation was more appropriate.

Vickery (1986) updated the expressions for internal pressure by considering the flexibility of the building envelope. This was introduced as a ratio of the bulk air to the bulk modulus of the building. The Helmholtz frequency of the building, which is usually compared with the frequency of the wind in the windward direction, is another important factor. Table 2 gives a list of the development of different expressions for internal pressure. Holmes and Ginger (2012) presented a thorough review of the development of the theories, expressions and parameters used in determining internal pressures relating to a case of a dominant opening, while Oh et al. (2007) provided a summary of previous experimental studies and theoretical development on internal pressures from 1930 to 2003.

Based on these theories, Pearce and Sykes (1999) and Sharma and Richards (2003) extended the area of application of the theory to include the effects of oblique winds and flexible envelopes (roofs and walls), while others (Guha et al., 2011; Holmes and Ginger, 2012) used the theory to develop equations comparing the RMS of the internal pressure coefficient and external pressure coefficient in cases of dominant openings. Sharma (2012) noted a significant difference in the orifice loss coefficient (C_L) (which accounts for pressure losses caused by the entry and exit of air through the opening) and inertia coefficient (C_I) (it accounts for pressure losses caused by the expansion and contraction of the opening) used in several experimental and numerical research works on internal pressure where C_L ranged from 2.5 to 45 and C_I ranged from 0.7 to 1.55. These two coefficients are major parameters in determining the internal pressures (peak and fluctuating) in buildings with a dominant opening. Estephan et al. (2021) included a leakage area to volume parameter to the equation by Holmes (1979), to improve the prediction of internal pressures due to air leakage through defects in walls. To further improve the estimation of internal pressures using theoretical formulas and reduce the risk of roof failures, there would be a need to adopt accurate values for specific building configurations. This would require further investigations through accurate experimental (that include extra internal volumes in scaled models based on scaled wind velocity) and numerical studies.

3.2. Factors affecting the internal pressure in buildings

Studies on internal pressures have focused on the transient response, the steady-state response, or a combination of both. Factors affecting the internal pressures are discussed below.

3.2.1. Size of opening (dominant and background openings)

Openings in a building envelope include both background openings (often measured in terms of building porosity), and dominant openings (such as doors and windows). Ginger et al. (1997) and Ginger (2000)

defined dominant openings as openings greater than twice the total background leakage area. According to Vickery (1994), for estimating mean pressures, a dominant opening is one with an area that is at least three times the total background leakage area. Windward openings in a building envelope are those at which the external pressure drives air into the building (as shown in Fig. 6), thus increasing the internal pressure. The size of openings is therefore a major factor in determining the internal pressures. Sharma and Richards (2005) and Chowdhury et al. (2013) have shown that dominant openings are a major factor affecting net roof pressures in low-rise buildings.

While considering a non-porous model, Holmes (1979), Saathoff and Liu (1983), Ginger et al. (1997) and Ginger (2000) noted that internal pressure oscillation frequencies increase with the increasing dominant opening area, indicating higher effects of damping in smaller opening areas. This conclusion was confirmed by Oh et al. (2007), who considered a porous building. The coefficient of internal pressure has been derived as a function of the ratio of the area of windward wall opening (A_W) to the area of leeward wall opening (A_L) assuming conservation of mass. From studies of a nominally sealed building, Ginger et al. (1997), Ginger (2000) and Holmes (1979) concluded that the mean internal pressure coefficients (C_{p_i}) increases with increasing $\frac{A_W}{A_L}$ ratio while Ginger et al. (1997) and Humphreys et al. (2019a) noted that increasing the size of the windward wall opening leads to increased internal pressure as damping is reduced; the probability of occurrence of resonance then increases. Ginger et al. (2010) and Humphreys et al. (2019a) have shown that the ratio of opening area to entire room volume (S^*), a parameter obtained by multiplying two of the non-dimensional parameters considered by Holmes (1979), was a factor affecting the internal pressure.

Background porosity is a measure of opening/leakage that affects the internal pressure (Oh et al., 2007). Saathoff and Liu (1983) stated the difficulty of measuring or estimating the permeability/porosity of a building. In their study, they selected a building porosity (background leakage) between 0.0 and 3.0% based on existing literature as of 1983. Their results indicated that the internal pressures in buildings with low porosities were insensitive to wall openings greater than 5% of the wall area. Studies by Stathopoulos et al. (1979) indicated that there was a reduction in internal pressure with increasing porosity (53% reduction from 0 to 0.5% porosity, and 72% reduction from 0.5 to 3.0% porosity). From their experimental results, Stathopoulos et al. (1979) concluded that with wall openings larger than 20% of the wall area, the internal pressure coefficient did not depend significantly on the porosity of the building. The study by Oh et al. (2007) observed small or no effects on the internal pressure of a background opening of 7.1% of the main/-dominant opening while they observed such effects for background openings of 70% of the main/dominant opening. This is consistent with the suggestion of Vickery and Bloxham (1992) that the size of background openings only affects the internal pressures when it exceeds 10% of the main/dominant opening. Relating this to RTWCs loading, existing literature has shown that increasing the size of the openings in the building envelope leads to an increased internal pressure resulting in a higher net roof pressure, which increases the amount of wind loads transferred to the RTWCs. According to Chowdhury et al. (2013), this increase can be significant, where for a particular RTWC tested, there was a 300% increase in the peak net-uplift force coefficient.

3.2.2. Opening locations

Holmes (1979), Stathopoulos and Luchian (1989) and Vickery and Bloxham (1992) focused on the fluctuating and/or mean internal pressures in buildings with a single dominant opening at the centre of the wall. Beste and Cermak (1997), Ginger et al. (1997), Kopp et al. (2008), Sharma (2008), Sharma and Richards (2003) and Tecle et al. (2015) considered multiple dominant opening locations (i.e., centrally located, at building edges, and a distance from the centre). Kopp et al. (2008) showed that the mean internal pressure coefficients are higher with openings near the corner of the wall than with centrally located openings. Also, major fluctuations in internal pressure coefficients for openings toward the edges of the building occur at non-orthogonal angles of attack. In contrast, Oh et al. (2007) reported higher Helmholtz resonance pressure at wind directions normal to the opening.

Internal pressure is sensitive to the size of the opening when the opening is located on the windward side (Holmes, 1979; Stathopoulos et al., 1979; Habte et al., 2017). Liu and Rhee (1986) observed larger internal pressure fluctuations with openings at the leeward section of the building and attributed them to the turbulent wake generated by the building model, causing large fluctuations in external pressures at the leeward side. However, their model was rigid, with no leakages, and the flow conditions differed from those present in the atmospheric boundary layer. Internal pressure is insensitive to opening size and building porosity when the dominant opening is located at the leeward side and the windward side is sealed. With openings in both the windward and leeward sides of a building, the internal pressure is sensitive to the ratio of the areas of the windward opening to that of the leeward opening. The internal pressure coefficients increase with increasing ratio between the areas of the windward and leeward openings (Ginger et al., 1997). Chowdhury et al. (2013) concluded that the location of openings affects load distributions in RTWCs. Pfretzschner et al. (2014) made a similar observation for L-shaped buildings, where openings located at re-entrant corners caused higher uplift loads on building sides containing the opening. This effect can be further investigated in future studies.

3.2.3. Number of openings

Several studies (Holmes, 1979; Saathoff and Liu, 1983; Liu and Rhee, 1986) focused on a case of a single dominant opening in the windward and leeward sides of the building, while others (Ginger et al., 1997; Kopp et al., 2008; Oh et al., 2007; Sharma and Richards, 2003; Tecle et al., 2015; Vickery and Bloxham, 1992) considered dominant openings and background leakage.

To the authors' knowledge, Habte et al. (2017) performed the only study that considered progressive multiple wall openings while including background leakage. That study did not report internal pressures but rather the effective contribution of the internal pressures to the bending moments at the ridges and knees of a low-rise building frame. One of the reasons why multiple openings were not considered by other authors is that increasing the number of openings produces the same effect as increasing the area of a single opening. This assumption might not be correct as the location of openings affects internal pressures (Kopp et al., 2008). This is an area requiring more attention.

3.2.4. Opening geometry/shape

Most experiments involving internal pressures in buildings consider square or rectangular openings. However, Oh et al. (2007), Vickery and Bloxham (1992) and Alawode et al. (2022) considered a dominant circular opening, though no comparison was made between circular and rectangular shapes. Humphreys et al. (2019b) found that the opening shape had little effect on the loss coefficient, as they considered both square and circular background openings. Estephan et al. (2021) also found no significant effect of opening shape on the internal pressure coefficient while considering square and rectangular openings. Background leakages have usually been represented by having several circular holes in models, distributed over the surface of the model. Since analytical methods used in predicting internal pressures have shown the importance of the opening shapes, it would be beneficial to perform research into verifying existing shape parameters and developing new ones for various opening shapes.

3.2.5. Building volume

Holmes (1979) showed that an internal volume distortion is required in wind tunnel testing involving a scaled model to achieve a dynamically equivalent internal volume. His dimensional analysis shows that

$$V_{o,m} = V_{o,f} \frac{\left(L_m/L_f\right)^3}{\left(U_m/U_f\right)^2} \quad (2)$$

where L = geometric length, U = wind speed and V_o = internal volume and subscripts m = model scale and f = full scale.

This relationship has been used in experimental studies on internal wind pressure (e.g., Habte et al., 2017; Kopp et al., 2008). The volume of a building gives an indication of its damping capabilities. All other factors being unchanged, in a building with a large volume and small opening area, internal pressures have lower magnitudes whereas, in a structure with a small volume and large opening area, there is a higher chance of Helmholtz resonance (Kopp et al., 2008). The ASCE 7–22 Standard recognizes the effect of volume on internal pressures and recommends a reduction factor for partially enclosed buildings with large unpartitioned volumes in section 26.13.

Kopp et al. (2008) compared internal pressures in their model with those from National Institute of Standards and Technology (NIST) data (i.e., from (Ho et al., 2005)) having similar internal volume to opening area (V_o/a), dominant opening area to single wall area ($a/\ a_w$) and background leakage area to single wall area (a_l/a_w). After noting that the only difference in the models was the building size, it was concluded that the overall building size modifies the internal pressure by altering the fluctuations of the external pressure. The overall size of the building determines points of flow separation and re-attachment points, which affect the external pressures and ultimately affect the internal pressures. The study by Ginger et al. (2010) indicated a reduction in internal pressure coefficients (mean and peaks) with increasing volumes while opening areas are kept constant.

These studies indicated that RTWCs of buildings with larger internal volumes would likely experience lesser wind loads than buildings with smaller internal volumes, all other factors being the same. The reduction or increase of wind loads on RTWCs due to differences in internal volume still needs to be investigated as knowledge from this can be useful to design engineers, especially in lateral building expansion projects.

3.2.6. Building shape

Pfretzschner et al. (2014) used numerical models of low-rise buildings with rectangular and L-shaped plans to understand load paths in light-frame wood structures. The study found higher maximum uplift reactions in the walls of the L-shaped building compared to the walls of the rectangular building under similar uniform uplift roof pressure. Also, openings close to the re-entrant corner resulted in higher uplift force concentrations at the re-entrant corner than when the opening was at the side without re-entrant corners. The increase in maximum wall reaction under wind load from rectangular to L-shaped building was 33.64% in their research work.

Shao et al. (2018) compared wind pressure coefficients on 4:12-sloped hip roofs with L, T, and rectangular-shaped buildings. In comparison to rectangular plans, their study noted higher suction pressure coefficients in both T and L-shaped buildings at the roof eaves near the roof valley for oblique winds directed towards the roof valley.

It can then be inferred that the maximum uplift reaction at a RTWC due to wind loads in buildings with openings at re-entrant corners (i.e., L or T-shaped) would be higher than those with a rectangular shape.

3.2.7. Envelope flexibility of the building structure

Internal volume has an effect on internal pressures as discussed earlier. Kandola (1978) was one of the first to document this effect when he noticed an unexpected decrease in internal pressure in a sealed cube under varying wind directions. Such changes were attributed to the flexibility of the cube models used in the wind tunnel tests since one factor that could affect the internal volume of a building is the flexibility of its envelope. A flexible building envelope experiences a change in internal volume with changes in internal pressures.

Vickery (1986) noted a reduction in Helmholtz frequency as well as higher damping in flexible envelopes compared with a rigid building. Vickery (1986) then derived a method of accounting for the flexibility of the building envelope in the measurement of internal pressures. This method involved the use of an effective internal volume parameter (V_e) shown in Equation (3) instead of the internal volume of the flexible building (V_I).

$$V_e = V_I \times (1 + (K_A / K_B)) \quad (3)$$

where K_B is the building bulk modulus (ratio of increase in pressure to volumetric strain) and K_A is the bulk modulus of air.

The observation by Vickery (1986) is in agreement with the analytical solutions obtained by Sharma and Richards (1997), the experimental results obtained by Pearce and Sykes (1999), and the field observations of Fahrtash and Liu (1990). However, the analytical solutions indicate that the higher damping (due to envelope flexibility) alone does not explain the reduction of the resonant response, especially in the case of a flexible roof, where the internal pressure exhibits double resonance. Since envelope flexibility can be difficult to estimate, one method used by Ginger (2000) was pressurizing the building and measuring deflections at various points within it. This deflection was then used to calculate an effective internal volume based on the equations of Vickery (1986).

Sharma (2008) took the analytical work a step further by considering the effects of external pressure on the flexible roof component. The results agree with previous work, thus reinforcing the understanding that building flexibility contributes to damping the fluctuations of internal pressure. The roof of many tropical buildings are more flexible than the walls (Sharma, 2008); this provides an explanation for the susceptibility of flexible buildings to damage during high wind events. With respect to RTWCs, the high flexibility of building envelopes would increase the wind loads on the RTWCs, but no relevant quantitative information is available.

3.2.8. Characteristics of external pressure

Internal pressure fluctuations are induced by external pressure fluctuations (Ginger, 2000; Holmes, 1979; Humphreys et al., 2019b; Liu and Rhee, 1986; Pearce and Sykes, 1999). Sharma (2008) showed that there is a high correlation between roof external pressure and internal pressure. This correlation increases with roof flexibility. The mean, rms and peak internal pressures increase with the turbulence intensity especially in suburban terrain (Oh et al., 2007). Stathopoulos et al. (1979) observed higher coefficients of internal pressures in urban (built-up) exposures than those in open country exposure. Holmes and Ginger (2012) and Liu and Rhee (1986) noted the dependence of Helmholtz resonance in internal pressure fluctuations on the turbulence in the approach and wake flows. However, with respect to oblique winds, Sharma and Richards (2003) noted that eddy dynamics at the openings in a building are responsible for the high excitation of the internal pressures, rather than the turbulence in the external flow.

3.2.9. Compartmentalization of the building

Compartmentalization is the separation of the internal volume of a building into separate smaller volumes or rooms. Saathoff and Liu (1983) classified multi-room buildings as loosely connected or tightly connected. In loosely connected rooms, internal pressure is similar in all the rooms while in a building with tightly connected rooms internal pressure varies from room to room. This is because in a tightly connected room system, each room acts as an individual volume unit and if an opening exists in that room, the internal pressures respond based on its volume rather than on the entire volume of the building. Kopp et al. (2008) found that separating the attic from the living space results in lower internal pressure in the attic. Their study noted that as little as a 0.4% opening could result in a pressure equalization between the two compartments (i.e., 80% of peak pressures transmitted).

Saathoff and Liu (1983) used the equation they derived for

Table 3
Implication of internal pressure parameters on RTWCs.

Parameter	General conclusion/inference of effect on RTWC	References
Size of opening	The larger the windward opening the higher the internal pressures, translating in higher loads on the RTWCs. The larger the ratio of the area of windward to leeward opening, the larger the internal pressures, meaning larger pressures on RTWCs, especially in form of uplifts.	Ginger et al. (1997); Holmes (1979); Ginger et al. (1997); Ginger (2000); Humphreys et al. (2019a)
Location of opening	RTWC in some locations on the roof might experience higher loads due to openings in the building envelope	Beste and Cermak (1997); Ginger et al. (1997); Sharma and Richards (2003); Kopp et al. (2008); Sharma (2008); Tecle et al. (2015), Chowdhury et al. (2013) Feng et al. (2020)
Number of openings	The effect of having more number openings might not be the same as having a larger dominant opening area. Though increasing dominant opening sizes and the number of openings would increase internal pressures when located on windward sides of the envelope.	Kopp et al. (2008)
Geometry of opening	The effect is insignificant.	Humphreys et al., 2019b; Estephan et al., (2021)
Volume of building	The larger the volume of the building, the lower the magnitude of internal pressures when opening sizes are constant. This implies that RTWCs in buildings with large volumes experience lesser pressures due to uplift in comparison with buildings with low volumes.	Ginger et al. (2010)
Shape of building	In buildings with openings at re-entrant corners, the internal pressures are higher in comparison with those with rectangular or square plan shapes	Pfretzschner et al. (2014)
Envelope flexibility of the building structure	Envelopes with high flexibility experience a reduction in Helmholtz frequency and higher damping. It can hence be inferred that RTWCs in buildings with envelopes having high flexibility would experience higher wind loads.	Ginger (2000); Sharma (2008)
Characteristics of external pressure	External pressure influences internal pressures, especially in buildings with openings. RTWCs in buildings located in areas of high-velocity winds or turbulent winds will hence experience higher wind loads.	Liu and Rhee (1986); Holmes (1979); Pearce and Sykes (1999); Ginger (2000); Humphreys et al. (2019b)
Compartmentalization of building	In rigidly compartmentalized buildings, internal pressures are limited to compartments with external openings hereby causing higher internal pressures in that compartment resulting in higher uplift loads for RTWC in the compartmentalized section. In loosely compartmentalized buildings the internal pressures vary the same, causing an almost fair sharing of uplift members across all RTWCs present.	Saathoff and Liu (1983)

multi-room systems to develop a Computer Systems Modelling Program (CSMP) for simulating different multiple-room scenarios with no leeward opening. In a 2-room building, when one of the rooms is completely sealed, the internal pressure fluctuates based on the volume of the room with the windward wall opening. However, if there is an opening between the two rooms that is larger than the windward wall opening, the internal pressures in both rooms fluctuate with similar frequencies but are out of phase. The fluctuations in both rooms are similar to the expected fluctuations if both rooms were combined (with no separation). This is different from the case in which the windward wall opening area is equal to the opening between the two rooms. Both studies concluded that internal pressures can be increased due to a reduction in volume as a result of compartmentalization.

With respect to RTWCs, smaller compartments with external openings would have more vulnerable RTWCs in comparison to larger compartments based on the findings described above. Table 3 gives a summary of the parameters and general conclusions regarding RTWCs.

4. Experimental, numerical, and analytical studies on RTWC wind loading

In the study of the effects of wind loads on RTWCs, researchers have employed experimental, numerical, and analytical methods either separately or in combination.

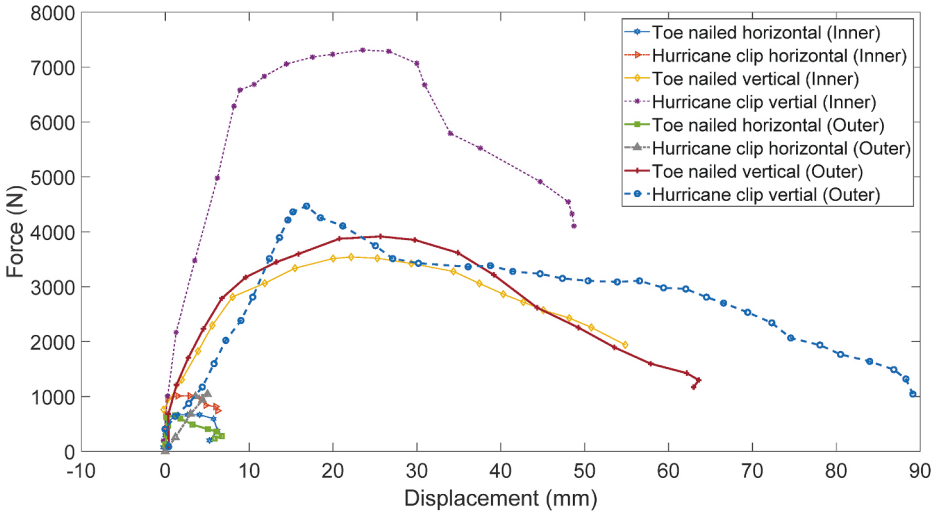

Fig. 7. Force-Displacement response of different RTWCs to different load types (Riley and Sadek, 2003).

Table 4
Previous experimental studies on RTWC's.

References	RTWC Types/ Roof Type/Scale	Failure Types	Test Methodology	Loading Considerations	Comments
Conner et al. (1987)	Toe nailed a. 3 16d nails (L-Type) b. 2- 16d +3-16d nails (M-Type), c. 3-16d and 8-in log bolts (H-Type) d. Clip angles e. Strapping Structural Scale-1:1	Nail withdrawal, rafter split, angle bent, bolt pull out, top plate collapsed and bolt pulled through the washer	Uplift loads applied using hydraulic rams	Static wind loads from ANSI A58.1 (1982), using GCp values and various wind speeds Dead loads were not considered	**Timber type** – Douglas Fir. The study presented a roof strength graph and experimentally showed that the H-type could withstand wind speeds of 110–180mph, the M-type can withstand 70-120mph and the L-type can only withstand 50-90mph wind speeds.
Reed et al. (1997a)	a. Toe nailed (3 8d nails), b. Metal connector (hurricane strip), c. Adhesives Component testing and Sectional tests 3:12 roof slope Structural Scale-1:1	Nail withdrawal, strap tear, rafter split, adhesive failure and wood fiber failure	Hydraulic jack for uplift loading using Spread beam (equal displacement) and load tree (equal loads on all)	Wind loads calculated from ASCE 7–93 with an assumed roof dead load, applied as static uplift loads	**Timber type** – Southern yellow pine and Spruce pine fir. Toe-nailed connections have a lower uplift capacity in comparison to hurricane straps. However, the straps provided no major load sharing. The study developed a design capacity chart based on individual connection tests.
Riley and Sadek (2003)	3-16d nails (Toe nailed) Hurricane clips Gable roof with a 3:8 slope Structural scale-1:1	Nail withdrawal and The top plate pulled from the wall	Uplift loads were applied using hydraulic rams. a monotonic uplifts, b monotonic lateral and. c cyclic lateral loads. d. combined uplift and lateral	Uplift capacity was the focus. The ratio of lateral to uplift loads was only assumed for a strong windstorm	**Timber type** – Spruce pine fir timber Nonlinear behavior of both toe-nailed and hurricane strap connections Uplift failure governs the failure in the uplift and shear load scenario Toe-nailed connections have a lower uplift capacity in comparison to hurricane straps.
Shanmugam et al. (2009)	Toe nailed a 2-16d nails. b. 3-16d nails. c. 3-8d nails. Gable roof; Sectional test. Structural Scale-1:1	Nail withdrawal and joist wood split	Monotonic and cyclic loads were applied using screw jacks	Uplift capacity was the focus. Roof dead loads were considered. ASTM D1761D 1761(2020) component testing protocol was used	**Timber type** – Southern yellow pine Toe-nailed connections are unsafe in high-wind areas. The 3-nail system had a 30% higher uplift capacity compared with the 2-nail system.
Ahmed et al. (2011)	Hurricane clips (1,2 and 4 clips per joint), Component Testing Structural Scale-1:1	Nail withdrawal, top plate rupture, rafter rupture, deformation of clips and clip tear	Uniaxial loading was applied with a Universal testing machine with a rig	Uplift capacity was the focus. Load rates were applied following the ASTM D 1761 protocol.	**Timber type** – Spruce pine fir, southern yellow pine, and Douglas fir wood Connection capacity is not directly proportional to the number of fasteners used (not additive), Developed an equation for the capacity calculation when using more than one clip.
Shanmugam et al. (2011)	a. Flat plate, b. Hurricane clip and c. Hurricane straps Component testing Structural Scale-1:1	Strap tear, Top plate slip, nail withdrawal from the top plate, buckling and nail withdrawal from rafter	Loads were uniaxial, biaxial and triaxial using a reaction frame	Load rates were applied following the ASTM D 1761 protocol, Different uplift to lateral load ratios were applied.	The study addressed multi-axis loading. The authors proposed the use of design loads that are 75% of connector capacity in a given load direction The study showed that the interaction design formula currently used in practice is overly conservative
Morrison and Kopp (2011)	Toe-nailed (3-12d nails) Component testing Gable Roof with 4:12 slope Structural Scale - 1:1	Withdrawal of nail and rafter wood split	Ramp and realistic wind loads were applied using Pressure loading actuators (PLA).	Only withdrawal loads (Uplift) using Wind Tunnel (WT) generated loads from a 1:50 scale testing.	**Timber type** – Douglas Fir-Larch The failure capacity of connectors is independent of the loading rate. The maximum load applied during realistic wind loads (fluctuating) was higher than the failure capacity measured from ramp loading (static).
Canino et al. (2011)	a. Hurricane clips b. FRP glass Component testing Plan –square Gable Roof with 4:12 slope	Nail withdrawal, clip rupture, fracture of wood and detachment of wood surface.	Triaxial loading and uniaxial loading using hydraulic jacks	Triaxial loading was based on data obtained from full-scale wind loading tests for a. closed b. partially enclosed and c. rain effects	**Timber type** – Spruce pine fir FRP ties performed better than the Hurricane clip. Unidirectional component tests overestimate the capacity of connectors subjected to aerodynamic loads.

(*continued on next page*)

Table 4 (*continued*)

References	RTWC Types/ Roof Type/Scale	Failure Types	Test Methodology	Loading Considerations	Comments
	Structural Scale - 1:1				
Morrison et al. (2012)	Toe Nailed (average of 3 per connection) Plan –square Entire roof testing Gable Roof with 4:12 Slope Structural Scale - 1:1	Nail withdrawal	Ramp and realistic wind loads were applied using PLA	Only withdrawal loads (Uplift) using Wind Tunnel (WT) generated loads from a 1:50 scale testing.	The study suggested that both individual components and entire roof tests show the incremental failure of connections. It would take longer duration storms (i.e., multiple peak loads) to cause complete failure of the toe-nailed connections in an entire roof system as compared with a few peak loads that cause the failure of single connections in component testing. The effective tributary area for each connection is larger than the nominal tributary area indicating considerable load sharing. Shear loads were not included.
Edmonson et al. (2012)	a. Flat plate connector b. Toenails (2-16d) Component testing Structural Scale - 1:1	Strap tear, top plate split, rafter wood split and nail withdrawal	Monolithic loading (Uniaxial uplift, in-plane, and out-of-plane loads) was applied separately on aged and new wood using a reaction frame.	Focused on uplift capacity checks (testing to National Design Specification (NDS) (AF&PA, 2005) and ASTM D1761)	**Timber type** - Aged and new Southern pine Aged timber has less capacity in comparison to new timber Uplift and out-of-plane capacities are additive (combining two types of connectors) but not the in-plane capacity
Chowdhury et al. (2013)	Hurricane clips Component testing Plan -square Gable roof with 4:12 slope Structural Scale - 1:1	None (Not within the scope of testing)	Peak force coefficients from a WT test on a full-scale roof with enclosed and partially enclosed walls were measured.	Triaxial aerodynamic loads obtained from WT studies were applied on individual connections using a reaction frame	**Timber type** - Spruce pine fir Redistribution of load was not considered. The study reported a more than 400% increase in net-uplift force coefficient due to openings in building envelop and higher internal pressure.
Satheeskumar et al. (2016b)	Triple grip connector Plan -square Gable roof with 4.7:12 slope Structural Scale - 1:1	None (Not within the scope of testing as loading was within serviceability limits)	Static loads were applied normal to the roof using a hydraulic ram	Static loads were applied ranging from 0.7 kN to 1 kN	Roof lining elements such as ceilings contribute to load sharing. RTWCs are most vulnerable to high uplift wind loads at roof eaves
Feng et al. (2020)	Flat plate connector Plan -Rectangular Gable Roof with 3:12 Slope Structural Scale - 1:1	None	Wind tunnel tests (1:4 length scaled building) using hurricane winds while considering closed and two partially enclosed cases	Wind tunnel tests using hurricane winds	The scaling of structural properties was not considered Uplift forces on the roof were higher for the partially enclosed cases. The location of openings had less effect on individual loading on connections near the gable end.

*Sectional tests refer to tests on a section of the roof.
*Component tests refer to tests on a single roof-to-wall connector.
*Structural scale refers to the scaling of the roof-to-wall connector's properties.

4.1. Experimental studies on RTWCs

Experimental studies on RTWCs can be classified into two groups; Performance/Capacity of different types of RTWCs (Ahmed et al., 2011; Canino et al., 2011; Edmonson et al., 2012; Morrison and Kopp, 2011; Reed et al., 1997a; Satheeskumar et al., 2016b), and Load distribution in a system of RTWCs (Morrison et al., 2012; Satheeskumar et al., 2016a). Studies by Conner et al. (1987) and Reed et al. (1997b) using monotonic uplift loads indicate that hurricane straps perform significantly better than nailed connections. A NIST study (Riley and Sadek, 2003) considering cases of monotonic lateral loads, monotonic uplift loads, a combination of lateral and uplift loads and cyclic lateral loads concluded that hurricane straps perform significantly better than nailed connections. Fig. 7 shows a comparison of hurricane straps and toe-nailed connection force-displacement response to horizontal/lateral loads and uplift/vertical loads, from tests by Riley and Sadek (2003). In Fig. 7 'inner' refers to RTWC away from the roof edge and 'outer' refers to RTWC at roof edge. The results shown in Fig. 7 indicate higher displacements in edge/outer RTWCs (both toe-nailed and hurricane strap) in comparison to non-edge/inner RTWCs for similar loads. The uplift capacity of some types of RTWC depends on the type of nailing method (i.e., hand nails or gun nails), variation in timber type, and missing nails (Satheeskumar et al., 2016b).

The classification of the experimental studies of RTWCs can also be based on the type of load considered in each study. On this basis, experimental studies can be classified into dynamic wind-loading groups and no-wind-loading groups. Most studies in the no-wind-loading groups have used monotonic loadings either based on the authors' judgment or on testing standard protocols (e.g., ASTM D 1761). Table 4 provides a summary of experimental tests conducted on RTWCs.

Under high wind loads, RTWCs are subjected to tri-axial loads (i.e., uplift, in-plane, and out-of-plane loads). While this is the case, most RTWC tests prior to Riley and Sadek (2003) used uni-axial loads, which resulted in the overestimation of the capacity of RTWCs (Shanmugam et al., 2011; Canino et al., 2011). The study by Riley and Sadek (2003) considered both uni-axial and bi-axial loading on RTWCs using an

estimated 0.295 ratio between the uplift and lateral loads. Uni-axial, bi-axial and tri-axial loading performance checks on RTWCs were conducted on three types of hurricane clips (also referred to as metal connectors) by Shanmugam et al. (2011) using monotonic loads. The study proposed a generalized design surface to be used in the design of metal connectors. While this was a step in the right direction, it should be noted that the loading used in the tests did not represent realistic wind loads.

Canino et al. (2011) carried out tri-axial load performance tests on a metal connector and a fiber-reinforced polymer (FRP) connector using loads obtained from a wind tunnel test. The study indicated a comparable performance of the FRP and the metal connector. Both Morrison et al. (2012) and Chowdhury et al. (2013) used aerodynamic loads for the performance checks of nailed connections and metal connectors, respectively. However, only the study by Chowdhury et al. (2013) considered the effects of internal pressures when sections on the building envelope are open. The study showed up to a 300% increase in peak net-uplift force coefficients from enclosed to partially enclosed conditions.

Another basis for grouping experimental works on RTWCs is the model's component level. The three groups are: individual/single RTWC models (Ahmed et al., 2011; Canino et al., 2011; Edmonson et al., 2012; Morrison and Kopp, 2011; Reed et al., 1997b; Shanmugam et al., 2011), continuous roof and wall models/multiple RTWCs (Conner et al., 1987; Reed et al., 1997b; Riley and Sadek, 2003), and full building model groups (scaled or unscaled) (Shanmugam et al., 2009; Chowdhury et al., 2013; Feng et al., 2020). Fig. 8 shows typical experimental setups for both full-building models and single RTWC testing. Fig. 9 shows typical RTWC failures from previous research works. The full building models and continuous roof and wall connection models enabled researchers to investigate load sharing/distribution behaviors. This will be discussed further in Section 5.

4.2. Numerical methods on RTWCs

One of the advantages numerical models have over experimental tests is the ability to consider material properties and load changes at every location of the model, unlike in experimental tests where these properties are only determined at positions where sensors are placed. Another advantage is the large number of parametric cases and model shapes that can be tested in numerical methods without additional costs other than computation costs.

Numerical studies on RTWC can be classified based on model complexity as single unit models that simulate one joint (Satheeskumar et al., 2017a), roof-only models and full roof and wall system models (Satheeskumar et al., 2017b; He et al., 2018a). Fig. 10 shows numerical models of a single joint (with detailed modeling of the RTWC, nails and boundary conditions) and an entire building from previous research works. Satheeskumar et al. (2017b) indicate that the finite element models of RTWCs have a slightly higher uplift capacity and/or influence coefficient (in the range of 15%) compared to experimental tests. However, Satheeskumar et al. (2017a, 2017b) concluded that the models were reasonable. The reasons for this higher estimate of RTWC capacity in numerical studies are linked with the unchanging stiffness of the RTWC model under increased deformation, the use of RTWC with the same stiffness in all directions, unlike actual RTWC used in experimental tests, and the uncertainty inherent in the construction of experimental models. Satheeskumar et al. (2017a) noted a similar percentage overestimation (~50%) of uplift capacity of triple grip (hurricane) connectors with respect to the experimental tests by Chowdhury et al. (2013) as the triple grip connectors are only rated based on vertical loading tests in one direction. Limitations of numerical models are due to the paucity of information on nonlinear material properties of connections with various wood types and contact conditions (Kasal et al., 1994; He et al., 2018).

A few numerical models have shown promise, such as the numerical study by Stevenson et al. (2019), which indicates that toe-nailed connections are the weakest link in the roof truss (to wall connection), but with the use of hurricane straps, this changes to the top chord joint. Experimental tests by Riley and Sadek (2003) have also shown that failure mechanisms have included split top plate/chord in cases where hurricane clips are used. A numerical study by He et al. (2018) simulated the incremental failure/progressive withdrawal of nails in RTWCs, where the capacity to partially evaluate the duration effect of wind loads was included. Also, Dhakal and Parvin (2021) modeled component-level FRP connections that showed the glass FRP had 9.5 times the shear

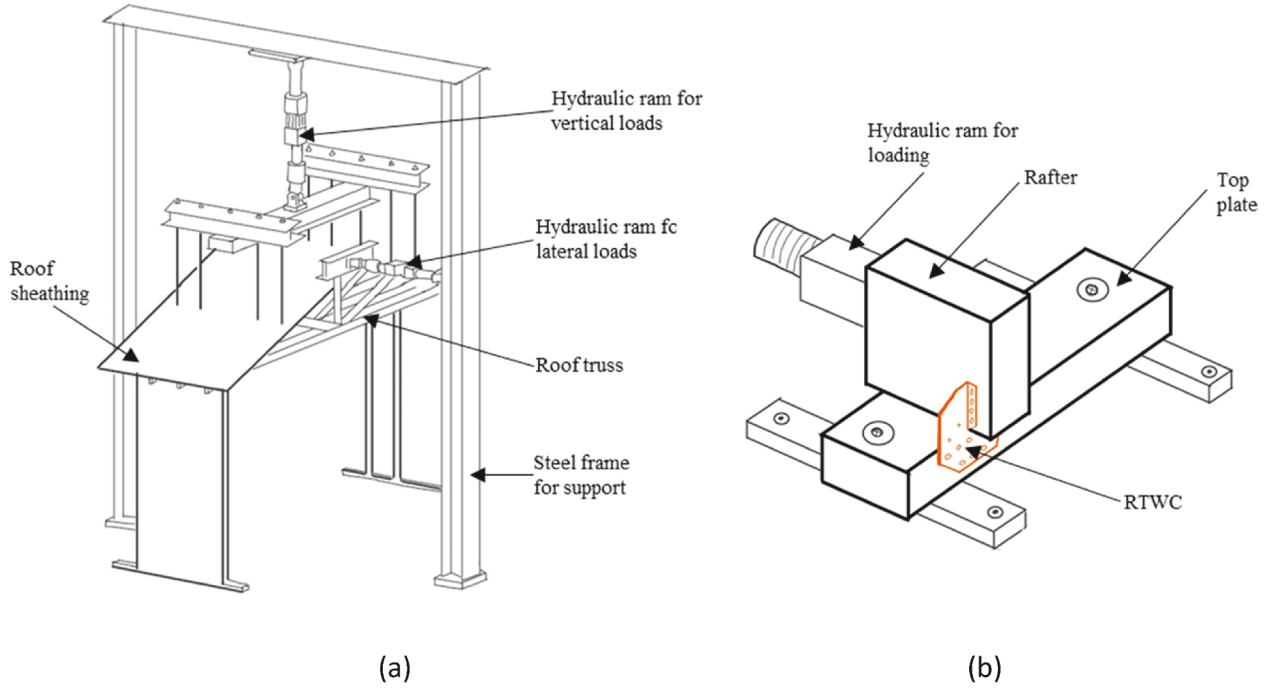

Fig. 8. Typical RTWC testing setup (a) full building (b) single RTWC

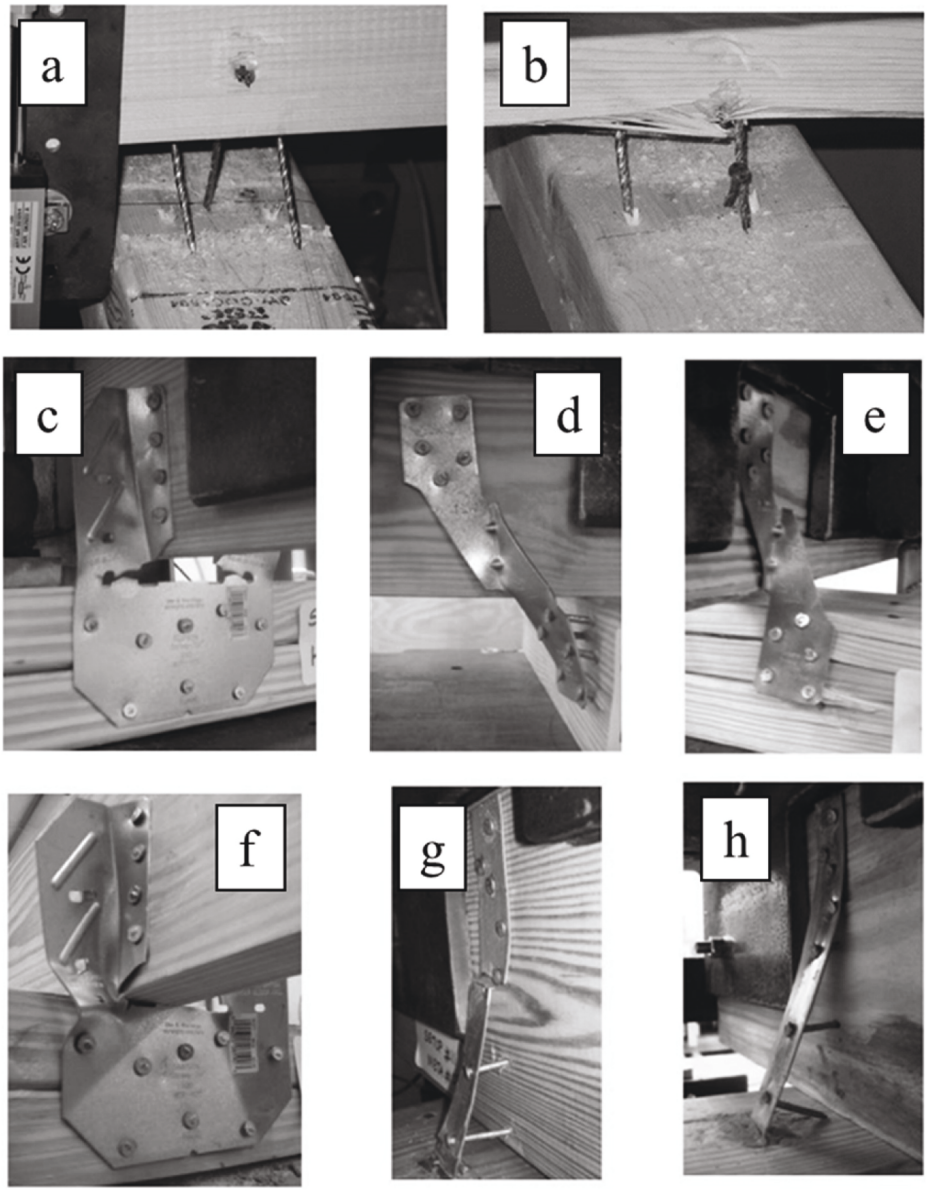

Fig. 9. Failures in RTWCs (a) Nail withdrawal in toe-nailed connection (b)Wood split and nail withdrawal in toe-nailed connection (c) Flat plate connector tear (d) Nail withdrawal from the top plate and hurricane connector (e)Top plate split (f)Flat plate connector buckling (g)Nail withdrawal and strap tear, and (h))Nail withdrawal from the rafter (reprinted from Morrison and Kopp, 2011 and Shanmugam et al., 2011).

capacity and 1.7 times the uplift capacity of hurricane clips. As regards the wood properties used in numerical models, wave propagation has been used to get the elasticity properties of wood by Kasal et al. (1994). Table 5 provides a summary of previous numerical studies on RTWCs under wind loading, indicating the numerical methods used.

4.3. Analytical models

Only a few studies have developed analytical models to estimate the wind capacity of RTWCs. Shanmugam et al. (2009) using displacement and reaction forces from a field/in-situ RTWC study developed an analytical model to evaluate the toe-nail-withdrawal failure of RTWCs. While this study utilized aged RTWCs, there was no comparison to new RTWCs, making it difficult to assess the influence of aging on the RTWC performance. The model by Shanmugam et al. (2009) adopted the unloading stiffness degradation model to account for the reduction in strength of the RTWC material over cyclic wind loading and for the simulation of the non-linear response as expected in realistic RTWCs.

Shanmugam et al. (2011) developed a design-based approach (based on allowable stress design methods) to estimate design capacities of metal RTWCs considering the multi-axis loading and behavior of three types of connectors. The authors identified four design scenarios (1st order surface, 2nd order surface, cuboid surfaces and a combination of 1st order and cuboid), and one was picked depending on a design space ratio obtained for each scenario.

Guha and Kopp (2014) developed both a nail slip model and a load sharing model for RTWCs. The nail slip model considered failure accumulation and was based on earlier component studies by the authors. The load sharing model only incorporated uplift loads with neither downward nor horizontal loads while simplifying the roof as a statically indeterminate continuous beam. The authors found good agreement between the models and existing experimental results. Table 6 gives further details of previous analytical studies on RTWCs.

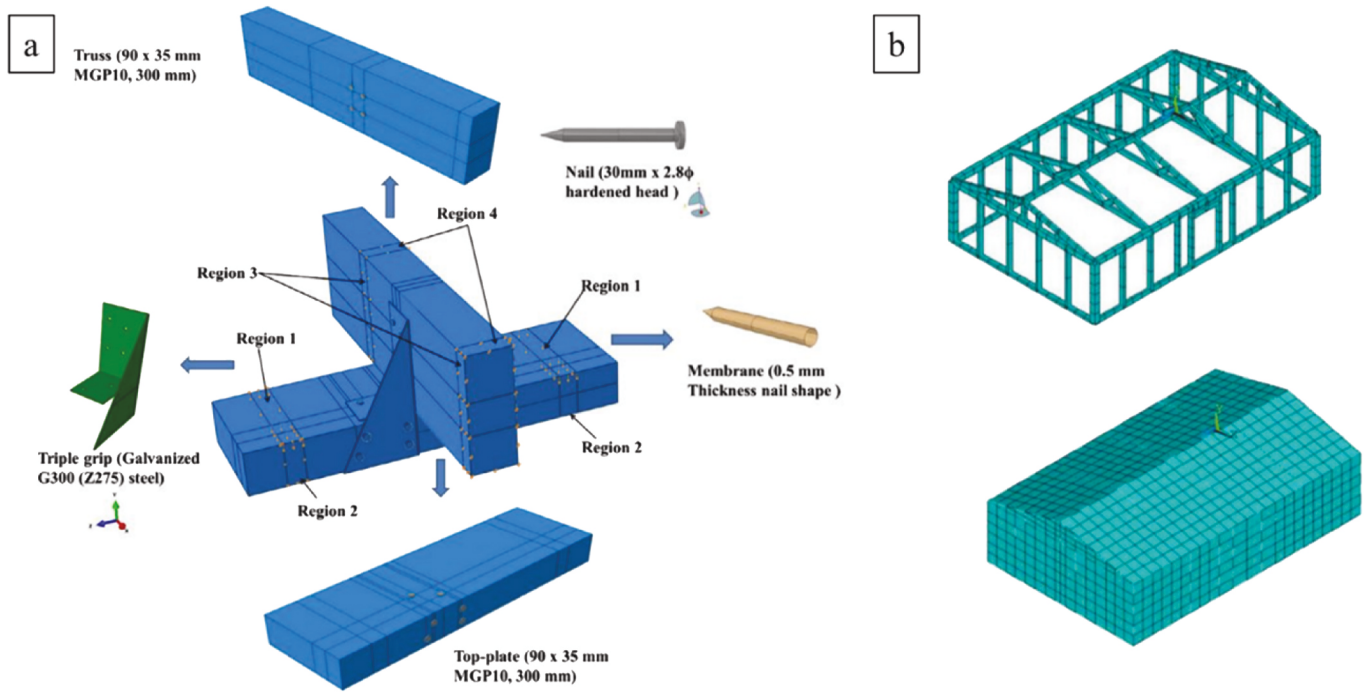

Fig. 10. Numerical model types (a) Single RTWC (b) Full building (reprinted from He et al., 2018 and Satheeskumar et al., 2017a).

5. Load sharing in RTWCs

Load sharing is the transfer of loads from weak connections to strong connections or from connections with more loading to those with less loading, through relative displacement (Henderson et al., 2013; Wolfe and LaBissoniere, 1991). Load sharing in components of timber-framed roofs such as RTWC is an important parameter required to determine the structural performance of timber-framed houses (Morrison and Kopp, 2011; Satheeskumar et al., 2016a). It has been observed that RTWCs in a complete roof system have a higher uplift capacity when compared to a RTWC acting individually (Reed et al., 1997a). This shows that load sharing helps to increase the resilience of RTWCs. Morrison and Kopp (2011) also noted the importance of load sharing in RTWC, although their study did not consider it. Parameters affecting the load sharing in RTWC include spacing of the roof trusses, RTWC stiffness (Morrison et al., 2012), sub-fascia, roof sheathing type (Morrison et al., 2012; Reed et al., 1997a) and the presence of ceilings (Satheeskumar et al., 2016a).

Influence functions/coefficients for the reaction at a support when a unit load is applied along the truss or adjacent trusses determine the extent of load sharing. These coefficients have been developed by Wolfe and McCarthy (1989), Wolfe and LaBissoniere (1991), and Mani and Thesis (1997), without considering displacement in the RTWC and using static point loads. Realistic fluctuating loading yields a different failure mode on toe-nailed RTWCs other than ramp/static loading does, as shown by Morrison and Kopp (2011). This resulted in questions on the ability of influence functions developed so far to predict load sharing in field RTWCs subjected to stochastic wind loads (Morrison et al., 2012). However, Henderson and Ginger (2011) concluded that static loads and realistic cyclone loads in metal cladding fasteners produce similar reaction coefficients. These conflicting conclusions might be due to the difference in material response since one case consists of a wooden roof with a toe-nailed connection while the other case is a metal cladding with bolts. It is therefore necessary to perform comparative studies on load sharing in RTWCs of metal roofs and other types of roofs using realistic wind loads and static loads.

The test results of Henderson et al. (2013) confirmed their 2012 hypothesis that influence coefficients change as the load fluctuates and as RTWCs yield. A study by Satheeskumar et al. (2016a) also indicated that changes in load due to load sharing have an impact on the influence coefficient. The study recommended that the influence on an RTWC of loads from adjacent trusses can be limited to two trusses at either side of the RTWC of interest. The load sharing in roof trusses of full-scale timber framed houses was examined by Satheeskumar et al. (2016a), who reported a 20% vertical load reduction at the loaded roof truss support with the addition of ceilings, ceiling cornice and wall lining. This is because these elements increase the weight of the roof system which counteracts uplift forces. The study also reported a high lateral load on RTWCs in the absence of ceiling cornice and wall lining. Fig. 11 shows the load sharing influence coefficients at truss B (i.e., along point LB to RB) reported by Satheeskumar et al. (2016a) when static loads are applied at different construction stages and locations on the roof. It indicates trusses further away from truss B have little effect on the loads experience by truss B. Table 7 shows previous studies that focused on load sharing in roof trusses with RTWCs.

While the studies on load sharing in RTWCs of a roof have been informative and have shed more light on the interaction of loads and their transfer within the roof structure, some cases have not yet been performed experimentally (i.e., T or L or U shaped roof with the determination of influence coefficients); also the influence coefficients generated in these experiments do not cover all types of roofs; some of the coefficients are dependent on the spacing of trusses, making it more difficult to produce a generalized influence coefficient approach. This indicates that more work needs to be done to fully understand the load transfer in RTWC systems.

6. Current standards, codes and design recommendations

6.1. Wind load standards

Several standards on wind loads on buildings currently exist, adopted in building codes by various jurisdictions. The ASCE 7–22 (2022) is currently adopted in the USA, and the Eurocode EN 1991-1-4:2005 is adopted in Europe (with most European countries having their specific Annex). Design codes for wind loads on structures have evolved over the years based on research findings and lessons from failures of buildings caused by wind events. However, the wind loading standards have no

Table 5
Previous numerical studies on RTWCs.

Reference	Representation of RTWC	Aim	Limitations	Comments
Satheeskumar et al. (2017a)	8 node linear brick element (C3D8R) was used to assemble the triple grip connector and nails	Developed Finite Element (FE) Model to predict the uplift capacity of RTWC with or without construction defects (missing nails)	Only one joint was modeled. Material non-linearity between the numerical model and experimental tests. Nail slip was not observed in the model, as it was observed in the experimental tests by (Satheeskumar et al., 2016b)	Loading of the joints and arrangement of the model was similar to the experimental tests by (Satheeskumar et al., 2016b). The single nail model used embedment functions by (Li et al., 2012). The authors used *Abaqus software*. A single missing nail could reduce the uplift capacity of the RTWC by up to 40%. Uplift capacity was 55% less when a combination of lateral and vertical loads was applied
Satheeskumar et al. (2017b)	8-node linear brick element (C3D8R) with the nails in the triple grip connector, modeled as well (with a nonlinear spring element used to represent the embodiment property of the timber-nail joint)	Predict structural response in both the elastic and post-elastic phase, model the influence of lining elements (ceiling, wall lining and ceiling cornice)	The stiffness of the RTWC was constant in the model which was not the case in the full-scale test by (Satheeskumar et al., 2016a). Also, stiffness deteriorations were not accounted for in the model.	*Abaqus Software* was used for the FEM analysis. Loading used is similar to the study by Satheeskumar et al. (2016a). RTWCs were modeled using properties (force-displacement) from (Satheeskumar et al., 2016a) and (Satheeskumar et al., 2017a), and validated with the experimental work in (Satheeskumar et al., 2016a). FEM reactions were 5–15% higher than experimental values due to differences in stiffness of RTWC modeled, variable construction method, non-consideration of reduced stiffness with nail withdrawal and material non-linearity.
He et al. (2018a)	Zero mass nonlinear spring elements (accounting for only the axial uplift capacity) were used to represent the Hurricane clip	Develop a 3D FE model to determine load paths in low-rise buildings under wind loading in the linear and non-linear phases.	Experimental validation tests did not include mechanical properties tests on the connections. Also, nail withdrawal was not simulated.	A multi-linear force-deflection relationship was used to model the RTWC, with the tension property from the work of (Riley and Sadek, 2003). The model was validated with deflection measurements from wind tunnel tests on a 1:4 length scale model. The rotational capacity of the wall stud connections has negligible effects on the RTWCs. Sheathing thickness is an important factor in envelop behavior.
He et al. (2018b)	Nonlinear spring elements using mechanics-based load-deformation characteristics were used to represent the Hurricane clip	Develop an FE model that could predict structural response under wind loading.	The pressures on the building model could not be updated with the addition of openings unlike in the experimental study. The authors also suggested a discrepancy in material properties adopted in the model could be the reason for the higher failure speed in the model. The paucity of data on material properties of hurricane clips.	The model captures the progressive withdrawal behavior in RTWC as observed in experimental studies. The authors used *ANSYS* software. The model assumes constant internal pressure. Dynamic wind loading input was used in the study. Properties from (Riley and Sadek, 2003) were used for the modeling of the hurricane ties. The model underestimated the displacement of RTWC.
Stevenson et al. (2019)	A combination of Pinned and rigid joints. Authors used both toe-nailed connection and hurricane strap.	Develop a modeling method that can be used to assess the failure of framing members and connections in wood-framed trusses due to wind loads.	Limited research on element-by-element metal-plate-connected (MPC) truss joints A 2D finite element model was used	The study developed a 2D FE model. The study used RTWC properties for toe-nailed connections from (Morrison and Kopp, 2011) and hurricane straps from (Ellingwood et al., 2004) (who picked the clip properties from the manufacturer's report). *SAP 2000 software* was used. Demand to Capacity ratios were found for the different RTWC types. Uplift load applied to the frame was calculated based on the directional procedure of ASCE 7–10 (115 km/h wind speed). It was found that toe-nailed connections were the weakest members of the frame.
Dhakal and Parvin (2021)	SOLID65 with a 6-node solid element	Predict the shear strength of FRP connectors	It was a component test	Basalt, Carbon, and Glass FRP connector component testing using monotonic cyclic loading. Shear strengths of glass FRP were higher in comparison to hurricane clips.

specific recommendations for RTWCs other than guidance on determining net pressure coefficients from external and internal pressure coefficients.

- ASCE 7–22 Standard

In determining the internal pressures within a building for design purposes, the ASCE 7–22 Standard recommends the classification of

buildings into enclosed, open, partially enclosed, or partially open based on comparisons of the opening area with the gross wall area in which the opening is located. Each wall in the building is assumed to be a windward wall in selecting the class of the building. The internal pressure coefficient (GC_{pi}) is then determined from Table 26.13–1 of ASCE 7–22. It should be noted that the values of GC_{pi} in Table 26.13–1 of ASCE 7–22 are based on the research of Stathopoulos et al. (1979) and Yeatts and Mehta (1993), as indicated in C26.13 of the code. The code makes provision for a reduction factor for partially enclosed buildings containing a single, unpartitioned large volume. The reduction equation is based on the work by Vickery and Bloxham (1992) and Irwin and Dunn (1994). Also, the code specifies the protection of glazed openings depending on the location of the building, and its risk category to avoid the impact of wind-borne debris. In cases of multiple classifications, the code specifies the worst loading conditions.

Regarding the design of RTWC, the ASCE 7–22 is not explicit about which design method is appropriate, since RTWCs can be regarded as a component belonging to the Component and Cladding (C&C) class or as a member belonging to the Main Wind Force Resisting System (MWFRS). This issue was raised by Morrison and Kopp (2011) regarding the ASCE 7-05 Standard, and Henderson et al. (2013) regarding ASCE 7–10. Henderson et al. (2013) suggest that the C&C loads should be used for the design of the RTWC. The study by Feng et al. (2020) indicates that force coefficients in RTWCs measured in a wind tunnel model are in-between the C&C recommendations and the MWFRS recommendations of ASCE 7–16 (2016), with the latter requiring a value closer to the measured force coefficients.

- EN 1991-1-4:2005

The Eurocode code (BS EN 1991-1-4:2005 +A1:2010 2011) determines the internal pressure coefficient by three methods based on the opening area. The first step is to determine if the building has a dominant face (i.e., with an opening area that is at least twice the area of openings in the remaining faces). Buildings with dominant faces have an internal pressure coefficient (C_{pi}) value given as a function of the external pressure coefficient (C_{pe}). The C_{pi} values for buildings with no dominant face are determined from a graph in Fig. 7.13 of the code, which represents a function of the ratio of the building height and depth (h/d) and the opening ratio (μ). The opening ratio is the ratio of the sum of areas of openings with a negative or zero C_{pe} to the sum of the areas of all openings. Other values are given for silos, chimneys, and vented tanks with small openings. The code gives a different provision for structures with a total opening area on at least two sides greater than 30% of the area of that side. It considers these as either canopy roofs or free-standing walls, and for these a net pressure coefficient (C_{pnet}) is provided.

The (BS EN 1991-1-4:2005 +A1:2010 2011) provides C_{pe} values for loaded areas of 1 m^2 and 10m ^{2} as $C_{pe,1}$ and $C_{pe,10}$, respectively. Regarding roofing elements, including RTWCs, the (BS EN 1991-1-4:2005 +A1:2010 2011) suggests the use of $C_{pe,1}$ values which are higher than the $C_{pe,10}$ values.

6.2. Materials testing standards

Building components such as RTWCs (e.g., nails, hurricane clips, and straps) have manufacturers' ultimate capacity listed on the items. For wood fasteners, the capacity is usually based on test procedures stipulated by ASTM D1761, with the latest version being ASTM D1761-20. Hurricane clips and strap manufacturers have their products tested and design values established per ASTM D7147-21 (2021) and evaluated by the International Code Council (ICC) Evaluation Service (ES) or a similar ES (Shanmugam et al., 2011). Selection of these RTWCs is then based on these capacities and the requirements of the building code in the location of the proposed building project, and the Wood-Frame Construction Manual (WFCM) for One and Two-Family Dwellings (AWC American Wood Council, 2018a).

The NDS 2018 (AWC American Wood Council, 2018b) for wood construction and the Special Design Provisions for Wind and Seismic (SDPWS) (AWC American Wood Council, 2021) are the latest guidance from the American Wood Council on the design of mechanical fasteners (i.e., RTWCs). Previous versions of the ASTM D1761 have been criticized for their inability to provide reliable testing for RTWCs.

6.2.1. Conclusions, challenges, and prospects of future studies

RTWCs are an integral part of roofing systems in many low-rise buildings and have been identified as one of the weak links in a structure under high wind loads. While they have received some attention mainly due to roof failures during high wind events, some knowledge gaps still exist regarding their performance under different wind conditions and roof configurations. A review of wind loading on RTWCs has been presented, with a focus on structural wind engineering aspects such as factors that affect these wind loads, load sharing in a roofing system, as well as current design recommendations. Research works to date have examined the capacity of different types of RTWCs, which loading type (i.e., uniaxial, biaxial or triaxial loads) best represents the loads RTWCs are subjected to in buildings, and numerical and analytical models that can predict the uplift capacity of RTWCs.

From this review the following prospects for future research have been identified:

Table 6
Previous analytical studies on RTWCs.

Reference	RTWC Type	Focus/Failure Mode	Software/Approach Used/Validation
Shanmugam et al. (2009)	Toe Nailed (2Nail and 3Nails connections)	Approximate the uplift behavior of toe nailed connections Nail Withdrawal, Splitting wood and a combination of both Error: 0.7–6.7%	Open Sees Pinching4 Material-Represent RTWC and captures reduced strength and stiffness Input parameters: Ultimate uplift capacity, initial secant stiffness and displacement at peak load Validation with experimental work
Shanmugam et al. (2011)	Flat plate connector, hurricane clip and hurricane strap	Developing a design surface for the multi-axis loading of RTWC Strap tear, wood split, nail withdrawal and buckling Error: Not stated	Monte-Carlo Simulation was used to obtain design and safety probabilities. Data from experimental RTWC response under different loading conditions were used to develop the model.
Guha and Kopp (2014)	Toe Nailed	Estimate effect of storm duration on RTWC failures. Nail-withdrawal/Nail-slip Error: 10%	2D beam element model that combines nail-slip and load sharing. Monte Carlo Simulation was used to investigate the impact of windstorm duration. Model was validated with experimental tests by Khan (2012).

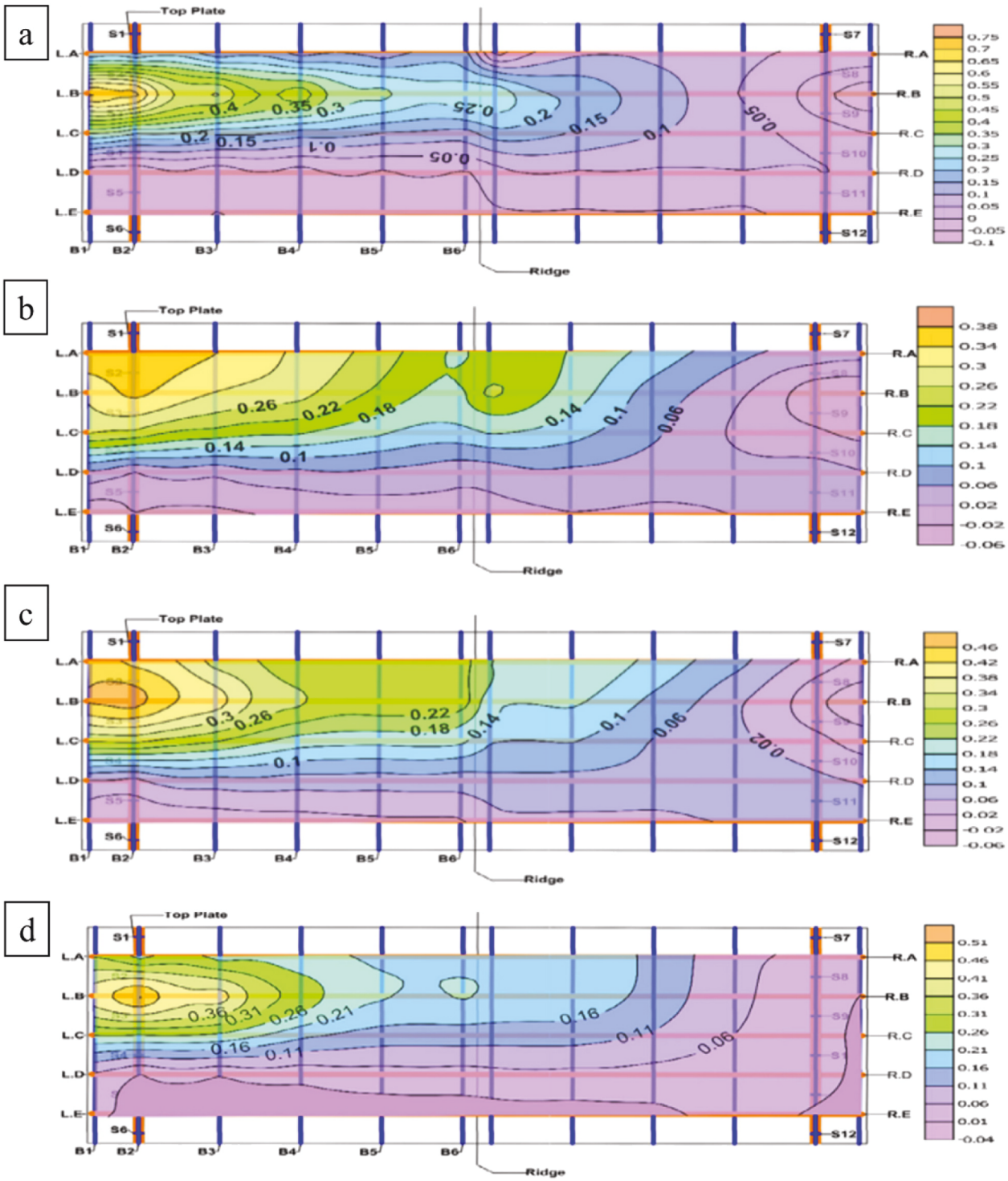

Fig. 11. Load sharing influence coefficients at truss B (a) Truss only (b) Trusses and battens (c) Trusses with battens and roof cladding (d) Trusses with battens, roof cladding and ceiling (reprinted from Satheeskumar et al., 2016a).

- Parametric study - Most experimental studies on RTWCs that consider realistic wind loads on buildings have used rectangular plan buildings with gable roofs and a 4:12 roof slope. There are no studies on buildings with different shapes (i.e., T-shape, etc.) and none on flat roofs related to RTWCs. Experimental tests on these other types of roofs could show interesting/different results in the load sharing and failure mode of their RTWCs, as roof slope affects the wind pressure distribution on the roof as well as load sharing.
- Another gap in the knowledge of realistic wind loading on RTWCs results from the absence of records of simulated wind profiles in the presence of surrounding buildings/structures. Higher wind turbulence in urban wind profiles could have a major impact on the damage/failure patterns and RTWC capacity.
- In terms of scaled models used in wind tunnel tests of RTWC capacities, there is a need to assess possible approaches to realistically simulate the properties of scaled RTWCs with reduced length scales and with the stiffness of roof truss materials. While scaling

Table 7
Previous studies on Load sharing in RTWCs.

Reference	Type of RTWC/ Roof Type	Failure Type	Loading Considerations	Study Type/Comments
Morrison et al. (2012)	Toe-nailed, Gable Roof	Nail Withdrawal	Loads from WT tests (on a rigid model) with a 40-degree wind direction were chosen for the study. Pressure-loading actuators (PLA) were used to load the roof. Internal pressure was not considered in the study.	Experimental tests. Incremental withdrawal of the RTWC at a joint change the load distribution across the roof. Loads on each truss which would translate to the RTWCs cannot be accurately calculated based on the simple tributary area method.
Henderson et al. (2013)	Toe-nailed (3 12d nails per joint), Hip Roof	Nail Withdrawal	Loads from WT tests (on a rigid model) with a 40-degree wind direction were chosen for the study. Pressure-loading actuators (PLA) were used to load the joint. WT tests simulated open country terrain. Nominally sealed building assumption with no dominant opening	Experimental tests. The influence area of a connection is larger than the nominal tributary area. Peak wind pressures that lead to nail or RTWC withdrawal also cause changes to load sharing.
Satheeskumar et al. (2015)	Triple grip metal connector – (Hip-End)	Not to failure	Uplift loads (1 kN) were applied at various sections of the roof.	Numerical study Wall lining, ceiling, and ceiling cornice increase the strength and stiffness of RTWCs External loads applied to the edges of the roof subject RTWCs to higher loads
Satheeskumar et al. (2016a)	Triple grip metal connector – (Hip End)	Not to failure	Static loads were applied 0.7–1 kN loads.	Experimental Static loads were applied as the authors believed that structural response under wind load is well represented by its response under static loads. Ceilings and ceiling cornice influence load sharing in roof systems. RTWC are vulnerable under high uplift loads applied to roof eaves.

connections can be very difficult/challenging, such tests would be more accurate and helpful in validating Finite Element models currently available.

- Although some studies suggest that static loading methods are unable to mimic actual failure modes of wooden connections. Developing an equivalent static and/or dynamic test method to assess the capacity of RTWCs could be a reliable alternative approach to wind tunnel testing. This would involve careful consideration of the multi-axis loading nature of wind actions on roofs of low-rise buildings. Such a test method, if adopted by manufacturers could help engineers design more resilient buildings.
- Currently, a general linear or non-linear loading response for different RTWC capacities under realistic wind loads with different load durations is not available. The absence of these data hinders the development of high-fidelity numerical models that can predict the performance of RTWCs in a roof under extreme wind conditions.
- Numerical modeling that can capture the behavior of RTWCs can be highly challenging due to computational time. No full study using updated wind loads on the changing building envelope (changes due to propagation of damage) has to our knowledge been performed. This is a path that in our opinion needs to be explored to better understand the progressive damage of RTWCs.
- The influence of aging of the RTWCs and the roof frames is yet to be considered in numerical research on RTWCs. Considering aging effects will enhance state-of-the-art numerical modeling. High fidelity numerical modeling will help to assess the vulnerability of low-rise light-weight wooden frame structures to better assist home-owners and insurance companies in the risk analysis of buildings subjected to wind loads.

CRediT authorship contribution statement

Kehinde J. Alawode: Writing – original draft, Conceptualization, Methodology. **Krishna Sai Vutukuru:** Writing – review & editing. **Amal Elawady:** Writing – review & editing, Supervision, Resources. **Arindam Gan Chowdhury:** Supervision, Resources.

Declaration of competing interest

The authors declare the following financial interests/personal relationships which may be considered as potential competing interests: Kehinde J Alawode reports financial support was provided by Florida Sea Grant.

Data availability

No data was used for the research described in the article.

Acknowledgments

The authors acknowledge the financial support provided by the NOAA-Florida Sea Grant (FSG) Program award #R/C-D-25. The contents expressed in this paper are the views of the authors and do not necessarily represent the opinions or views of FSG.

References

AF&PA (American Forest and Paper Association), 2005. National Design Specification for Wood Construction – ASD/LRFD in NDS. Washington, DC.

ASTM D1761, 2020. Standard Test Methods for Mechanical Fasteners in Wood and Wood-Based Materials. ASTM International, West Conshohocken, PA. https://doi.org/10.1520/D1761-20.

ASTM D7147, 2021. Standard Test Methods for Testing and Establishing Allowable Loads of Joist Hangers. ASTM International., West Conshohocken, PA.

American National Standards Institute (ANSI), 1982. Minimum Design Loads for Buildings and Other Structures. ANSI A58.1, New York, N.Y.

Ahmad, S., Kumar, K., 2002. Wind pressures on low-rise hip roof buildings. Wind and Structures, An International Journal 5 (6), 493–514. https://doi.org/10.12989/was.2002.5.6.493.

Ahmed, S.S., Canino, I., Chowdhury, A.G., Mirmiran, A., Suksawang, N., 2011. Study of the capability of multiple mechanical fasteners in roof-to-wall connections of timber residential buildings. Pract. Period. Struct. Des. Construct. 16 (1), 2–9. https://doi.org/10.1061/(ASCE)SC.1943-5576.0000064.

Alawode, K.J., Vutukuru, K.S., Elawady, A., Lee, S.J., Chowdhury, A.G., Lori, G., 2023. Wind-induced vibration and wind-driven rain performance of a full-scale single skin façade unit with Vertical Protrusions. J. Architect. Eng. 29 (2), 1–17. https://doi.org/10.1061/JAEIED.AEENG-1393.

Alawode, K.J., Vutukuru, K.S., Elawady, A., Lee, S.J., Chowdhury, A.G., Lori, G., 2022. Effects of permeability on the dynamic properties and weathertightness of double skin curtain walls. Proceedings of Structures Congress. https://doi.org/10.1061/9780784484180.038, 2022.

ASCE 7-93, 1993. Minimum Design Loads for Buildings and Other Structures. ANSI/ASCE Standard, Reston, VA.
ASCE 7-16, 2016. Minimum Design Loads for Buildings and Other Structures. ANSI/ASCE Standard, Reston, VA. https://doi.org/10.1061/9780872629042.
AWC (American Wood Council), 2018a. Wood Frame Construction Manual (WFCM) for One and Two-Family Dwellings. ANSI/AWC NDS-2018, Leesburg, VA.
AWC (American Wood Council), 2018b. National Design Specification for Wood Construction. ANSI/AWC NDS-2018, Leesburg, VA.
AWC (American Wood Council), 2021. Special Design Provisions for Wind and Seismic. ANSI/AWC SDPWS-2021, Leesburg, VA.
Azzi, Z., Habte, F., Elawady, A., Chowdhury, A.G., Moravej, M., 2020. Aerodynamic mitigation of wind uplift on low-rise building roof using large-scale testing. Frontiers in Built Environment 5, 1–17. https://doi.org/10.3389/fbuil.2019.00149.
Baskaran, A., Stathopoulos, T., 1988. Roof corner wind loads and parapet configurations. J. Wind Eng. Ind. Aerod. 29 (1–3), 79–88. https://doi.org/10.1016/0167-6105(88)90147-X.
Beste, F., Cermak, J.E., 1997. Correlation of internal and area-averaged external wind pressures on low-rise buildings. J. Wind Eng. Ind. Aerod. 69 (71), 557–566. https://doi.org/10.1016/S0167-6105(97)00186-4.
Blessing, C., Chowdhury, A.G., Lin, J., Huang, P., 2009. Full-scale validation of vortex suppression techniques for mitigation of roof uplift. Eng. Struct. 31 (12), 2936–2946. https://doi.org/10.1016/j.engstruct.2009.07.021.
BS EN 1991-1-4:2005 +A1:2010, 2011. Eurocode 1 - actions on structures Part 1-4: general actions — wind actions. BSI 86. https://doi.org/10.1680/cien.2001.144.6.14.
Canino, I., Chowdhury, A.G., Mirmiran, A., Suksawang, N., 2011. Triaxial load testing of metal and FRP roof-to-wall connectors. J. Architect. Eng. 17 (3), 112–120. https://doi.org/10.1061/(ASCE)AE.1943-5568.0000039.
Case, P.C., Isyumov, N., 1998. Wind loads on low buildings with 4:12 gable roofs in open country and suburban exposures. J. Wind Eng. Ind. Aerod. 77 (78), 107–118.
Chang, C.H., Meroney, R.N., 2003. The effect of surroundings with different separation distances on surface pressures on low-rise buildings. J. Wind Eng. Ind. Aerod. 91 (8), 1039–1050. https://doi.org/10.1016/S0167-6105(03)00051-5.
Chowdhury, A.G., Canino, I., Mirmiran, A., Suksawang, N., Baheru, T., 2013. Wind-loading effects on roof-to-wall connections of timber residential buildings. J. Eng. Mech. 139 (3), 386–395. https://doi.org/10.1061/(ASCE)EM.1943-7889.0000512.
Conner, H.W., Gromala, D.S., Burgess, D.W., 1987. Roof connections in houses: key to wind resistance. J. Struct. Eng. 113 (12), 2459–2474.
Dhakal, A., Parvin, A., 2021. Fiber reinforced polymer as wood roof-to-wall connections to withstand hurricane wind loads. CivilEng 2 (3), 652–669. https://doi.org/10.3390/civileng2030036.
Edmonson, W.C., Schiff, S.D., Nielson, B.G., 2012. Behavior of light-framed wood roof-to-wall connectors using aged lumber and multiple connection mechanisms. J. Perform. Constr. Facil. 26 (1), 26–37. https://doi.org/10.1061/(ASCE)CF.1943-5509.0000201.
Ellingwood, B.R., Rosowsky, D.V., Li, Y., Kim, J.H., 2004. Fragility assessment of light-frame wood construction subjected to wind and earthquake hazards. J. Struct. Eng. 9445 (April 2004), 1562–1569. https://doi.org/10.1061/(ASCE)0733-9445(2004)130.
Estephan, J., Chowdhury, A.G., Elawady, A., Erwin, J., 2021. Dependence of internal pressure in low-rise buildings on aerodynamic parameters, defect features and background leakage. J. Wind Eng. Ind. Aerod. 219, 104822 https://doi.org/10.1016/j.jweia.2021.104822.
Fahrtash, M., Liu, H., 1990. Internal pressure of low rise building - field measurements. J. Wind Eng. Ind. Aerod. 36, 1191–1200.
FEMA, 2005. Hurricane charley in Florida: observations. Recommendations, and Technical Guidance 488 (1), 1–24.
Feng, C., Chowdhury, A.G., Elawady, A., Chen, D., Azzi, Z., Vutukuru, K.S., 2020. Experimental assessment of wind loads on roof-to-wall connections for residential buildings. Frontiers in Built Environment 6, 1–14. https://doi.org/10.3389/fbuil.2020.00010.
Franchini, S., Pindado, S., Meseguer, J., Sanz-Andrés, A., 2005. A parametric, experimental analysis of conical vortices on curved roofs of low-rise buildings. J. Wind Eng. Ind. Aerod. 93 (8), 639–650. https://doi.org/10.1016/j.jweia.2005.07.001.
Gavanski, E., Kordi, B., Kopp, G.A., Vickery, P.J., 2013. Wind loads on roof sheathing of houses. J. Wind Eng. Ind. Aerod. 114, 106–121. https://doi.org/10.1016/j.jweia.2012.12.011.
Gerhardt, H.J., Kramer, C., 1992. Effect of building geometry on roof wind loading. J. Wind Eng. Ind. Aerod. 43, 1765–1773.
Ginger, J.D., Holmes, J.D., Kim, P.Y., 2010. Variation of internal pressure with varying sizes of dominant openings and volumes. J. Struct. Eng. 136 (10), 1319–1326. https://doi.org/10.1061/(ASCE)ST.1943-541X.0000225.
Ginger, J.D., Mehta, K.C., Yeatts, B.B., 1997. Internal pressures in a low-rise full-scale building. J. Wind Eng. Ind. Aerod. 72 (1–3), 163–174. https://doi.org/10.1016/S0167-6105(97)00241-9.
Ginger, J.D., 2000. Internal pressures and cladding net wind loads on full-scale low-rise building. J. Struct. Eng. 126 (April), 538–543.
Guha, T.K., Kopp, G.A., 2014. Storm duration effects on roof-to-wall-connection failures of a residential, wood-frame, gable roof. J. Wind Eng. Ind. Aerod. 133, 101–109. https://doi.org/10.1016/j.jweia.2014.08.005.
Guha, T.K., Sharma, R.N., Richards, P.J., 2011. Internal pressure dynamics of a leaky building with a dominant opening. J. Wind Eng. Ind. Aerod. 99 (11), 1151–1161. https://doi.org/10.1016/j.jweia.2011.09.002.
Habte, F., Chowdhury, A.G., Zisis, I., 2017. Effect of wind-induced internal pressure on local frame forces of low-rise buildings. Eng. Struct. 143, 455–468. https://doi.org/10.1016/j.engstruct.2017.04.039.
Harris, R.I., 1990. The propagation of internal pressures in buildings. J. Wind Eng. Ind. Aerod. 34, 169–184.
He, J., Pan, F., Cai, C.S., 2017. A review of wood-frame low-rise building performance study under hurricane winds. Eng. Struct. 141, 512–529. https://doi.org/10.1016/j.engstruct.2017.03.036.
He, J., Pan, F., Cai, C.S., Chowdhury, A.G., Habte, F., 2018. Progressive failure analysis of low-rise timber buildings under extreme wind events using a DAD approach. J. Wind Eng. Ind. Aerod. 182 (September), 101–114. https://doi.org/10.1016/j.jweia.2018.09.018.
He, J., Pan, F., Cai, C.S., Habte, F., Chowdhury, A.G., 2018a. Finite-element modeling framework for predicting realistic responses of light-frame low-rise buildings under wind loads. Eng. Struct. 164, 53–69. https://doi.org/10.1016/j.engstruct.2018.01.034.
He, J., Pan, F., Cai, C.S., Habte, F., Chowdhury, A.G., 2018b. Finite-element modeling framework for predicting realistic responses of light-frame low-rise buildings under wind loads. Eng. Struct. 164, 53–69. https://doi.org/10.1016/j.engstruct.2018.01.034.
Henderson, D.J., Ginger, J.D., 2011. Response of pierced fixed corrugated steel roofing systems subjected to wind loads. Eng. Struct. 33 (12), 3290–3298. https://doi.org/10.1016/j.engstruct.2011.08.020.
Henderson, D.J., Morrison, M.J., Kopp, G.A., 2013. Response of toe-nailed, roof-to-wall connections to extreme wind loads in a full-scale, timber-framed, hip roof. Eng. Struct. 56, 1474–1483. https://doi.org/10.1016/j.engstruct.2013.07.001.
Ho, T.C.E., Surry, D., Davenport, A.G., 1991. Variability of low building wind loads due to surroundings. J. Wind Eng. Ind. Aerod. 38 (2–3), 297–310. https://doi.org/10.1016/0167-6105(91)90049-3.
Ho, T.C.E., Surry, D., Morrish, D., Kopp, G.A., 2005. The UWO contribution to the NIST aerodynamic database for wind loads on low buildings: Part 1. Archiving format and basic aerodynamic data. J. Wind Eng. Ind. Aerod. 93 (1), 1–30. https://doi.org/10.1016/j.jweia.2004.07.006.
Holmes, J.D., 1979. Mean and fluctuating internal pressures induced by wind. In: 5th International Conference on Wind Engineerin, vol. 1. Pergamon Press Ltd, Fort Collins, Colorado, pp. 435–441. https://doi.org/10.1016/B978-1-4832-8367-8.50046-2.
Holmes, J.D., 1981. Wind Pressures on Houses with High Pitched Roofs. Wind Engineering Report 4/81. Department of Civil and Systems Engineering, James Cook University of North Queensland, Townsville, Australia.
Holmes, J.D., Ginger, J.D., 2012. Internal pressures - the dominant windward opening case - a review. J. Wind Eng. Ind. Aerod. 100 (1), 70–76. https://doi.org/10.1016/j.jweia.2011.11.005.
Humphreys, M.T., Ginger, J.D., Henderson, D.J., 2019a. Internal pressures in a full-scale test enclosure with windward wall openings. J. Wind Eng. Ind. Aerod. 189 (November 2018), 118–124. https://doi.org/10.1016/j.jweia.2019.03.024.
Humphreys, M.T., Ginger, J.D., Henderson, D.J., 2019b. Internal pressures in a full-scale test enclosure with windward wall openings. J. Wind Eng. Ind. Aerod. 189 (February), 118–124. https://doi.org/10.1016/j.jweia.2019.03.024.
Hussain, M., Lee, B.E., 1980. A wind tunnel study of the mean pressure forces acting on large groups of low-rise buildings. J. Wind Eng. Ind. Aerod. 6 (3–4), 207–225. https://doi.org/10.1016/0167-6105(80)90002-1.
Irminger, J.O.V., Nokkentved, C., 1930. Wind pressure on buildings. Experimental researches first series. Ingenior Videnskabelige Skrifter A Nr 23.
Irwin, P.A., Dunn, G.E., 1994. Review of internal pressures on low-rise buildings. RWDI Report 93–270.
Kandola, B.S., 1978. Wind effects on buildings with varying leakage characteristics - wind-tunnel investigation. J. Wind Eng. Ind. Aerod. 3 (4), 267–284.
Kasal, B., Leichti, R.J., Itani, R.Y., 1994. Nonlinear finite element model of complete light-frame wood structures. J. Struct. Eng. 120 (1), 100–119.
Khan, M.A.A., 2012. Load-sharing of toe-nailed, roof-to-wall connections under extreme wind loads. In: Wood-frame Houses (M.E.Sc. Thesis). The University of Western.
Kind, R.J., 1988. Worst suctions near edges of flat rooftops with parapets. J. Wind Eng. Ind. Aerod. 31 (2–3), 251–264. https://doi.org/10.1016/0167-6105(88)90007-4.
Kopp, G.A., Oh, J.H., Inculet, D.R., 2008. Wind-induced internal pressures in houses. J. Struct. Eng. 134 (7), 1129–1138. https://doi.org/10.1061/(ASCE)0733-9445(2008)134:7(1129).
Li, M., Foschi, R.O., Lam, F., 2012. Modeling hysteretic behavior of wood shear walls with a protocol-Independent nail connection algorithm. J. Struct. Eng. 138 (1), 99–108. https://doi.org/10.1061/(ASCE)ST.1943-541X.0000438.
Lin, J.X., Surry, D., Tieleman, H.W., 1995. The distribution of pressure near roof corners of flat roof low buildings. J. Wind Eng. Ind. Aerod. 56 (2–3), 235–265. https://doi.org/10.1016/0167-6105(94)00089-V.
Liu, H., 1975. Wind pressure inside buildings. In: Proceedings of the Third US National Conference on Wind Engineering, pIII-3-1, Fort Collins, Colorado, June 1975.
Liu, H., Saathoff, P.J., 1981. Building internal pressure: sudden change. J. Engrg. Mech. Div., ASCE 107 (2), 309–321.
Liu, H., Rhee, K.H., 1986. Helmholtz oscillation in building models. J. Wind Eng. Ind. Aerod. 24 (2), 95–115. https://doi.org/10.1016/0167-6105(86)90001-2.
Lythe, G., Surry, D., 1983. Wind loading of flat roofs with and without parapets. J. Wind Eng. Ind. Aerod. 11 (1–3), 75–94. https://doi.org/10.1016/0167-6105(83)90091-0.
Mani, S., 1997. Influence Functions for Evaluating Design Loads on Roof-Truss to Wall Connections in Low-Rise Buildings. M.S. Thesis. Clemson University, Clemson, South Carolina, United States.

Meecham, D., Surry, D., Davenport, A.G., 1991. The magnitude and distribution of wind-induced pressures on hip and gable roofs. J. Wind Eng. Ind. Aerod. 38 (2–3), 257–272. https://doi.org/10.1016/0167-6105(91)90046-Y.

Morrison, M.J., Henderson, D.J., Kopp, G.A., 2012. The response of a wood-frame, gable roof to fluctuating wind loads. Eng. Struct. 41, 498–509. https://doi.org/10.1016/j.engstruct.2012.04.002.

Morrison, M.J., Kopp, G.A., 2011. Performance of toe-nail connections under realistic wind loading. Eng. Struct. 33 (1), 69–76. https://doi.org/10.1016/j.engstruct.2010.09.019.

Oh, J.H., Kopp, G.A., Inculet, D.R., 2007. The UWO contribution to the NIST aerodynamic database for wind loads on low buildings: Part 3. Internal pressures. J. Wind Eng. Ind. Aerod. 95 (8), 755–779. https://doi.org/10.1016/j.jweia.2007.01.007.

Pearce, W., Sykes, D.M., 1999. Wind tunnel measurements of cavity pressure dynamics in a low-rise flexible roofed building. J. Wind Eng. Ind. Aerod. 82 (1), 27–48. https://doi.org/10.1016/S0167-6105(98)00213-X.

Pfretzschner, K.S., Gupta, R., Miller, T.H., 2014. Practical modeling for wind load paths in a realistic light-frame wood house. J. Perform. Constr. Facil. 28 (3), 430–439. https://doi.org/10.1061/(ASCE)CF.1943-5509.0000448.

Pierre, L. M. St, Kopp, G.A., Surry, D., Ho, T.C.E., 2005. The UWO contribution to the NIST aerodynamic database for wind loads on low buildings: Part 2. Comparison of data with wind load provisions. J. Wind Eng. Ind. Aerod. 93 (1), 31–59. https://doi.org/10.1016/j.jweia.2004.07.007.

Pindado, S., Meseguer, J., 2003. Wind tunnel study on the influence of different parapets on the roof pressure distribution of low-rise buildings. J. Wind Eng. Ind. Aerod. 91 (9), 1133–1139. https://doi.org/10.1016/S0167-6105(03)00055-2.

Pinelli, J.P., Roueche, D., Kijewski-Correa, T., Plaz, F., Prevatt, D., Zisis, I., l Elawady, A., Haan, F., Pei, S., Gurley, K., Rasouli, A., Refan, M., Rhode-Barbarigos, L., Moravej, M., 2018. Overview of damage observed in regional construction during the passage of hurricane Irma over the state of Florida. In: Proceedings of Forensic Engineering 8th Congress. American Society of Civil Engineers (ASCE), Austin. https://doi.org/10.1061/9780784482018.099.

Prevatt, D., Kameshwar, S., Roueche, D., Rittelmeyer, B., Duarte, T., Ibrahim, H., Klepac, S., Lafontaine, O., Lin, T., Manuel, L., Pilkington, S., Pinyochotiwong, Y., Santiago-Hernandez, J., Strader, S., Gurley, K., Kijewski-Correa, T., Mosalam, K., Robertson, I., 2021. STEER: Hurricane Ida Joint Preliminary Virtual Reconnaissance Report - Early Access Reconnaissance Report (PVRR-EARR). https://doi.org/10.17603/ds2-w6km-fe51.

Reed, T.D., Rosowsky, D.V., Schiff, S.D., 1997a. Uplift capacity of light-frame rafter to Top Plate connections. J. Architect. Eng. 3 (4), 156–163. https://doi.org/10.1061/(ASCE)MT.1943-5533.0000492.

Reed, T.D., Rosowsky, D.V., Schiff, S.D., 1997b. Uplift capacity of polyurea-coated light-frame rafter to Top Plate connections. J. Architect. Eng. 3 (4), 156–163. https://doi.org/10.1061/(ASCE)MT.1943-5533.0000492.

Riley, M.A., Sadek, F., 2003. Experimental Testing of Roof to Wall Connections in Wood Frame Houses (Gaithersburg, MD).

Saathoff, P.J., Liu, H., 1983. Internal pressure of multi-room buildings. J. Eng. Mech. 109 (3), 908–919. https://doi.org/10.1061/(ASCE)0733-9399(1983)109:3(908).

Satheeskumar, N., Henderson, D.J., Ginger, J.D., Humphreys, M.T., Wang, C.H., 2016a. Load sharing and structural response of roof–wall system in a timber-framed house. Eng. Struct. 122, 310–322. https://doi.org/10.1016/j.engstruct.2016.05.009.

Satheeskumar, N., Henderson, D.J., Ginger, J.D., Wang, C.H., 2016b. Wind uplift strength capacity variation in roof-to-wall connections of timber-framed houses. J. Architect. Eng. 22 (2), 1–12. https://doi.org/10.1061/(ASCE)AE.1943-5568.0000204.

Satheeskumar, N., Henderson, D.J., Ginger, J.D., Wang, C.H., 2017a. Finite element modelling of the structural response of roof to wall framing connections in timber-framed houses. Eng. Struct. 134, 25–36. https://doi.org/10.1016/j.engstruct.2016.12.034.

Satheeskumar, N., Henderson, D.J., Ginger, J.D., Wang, C.H., 2015. Wind loading effects on roof to wall connection in a timber frame structure. In: 14th International COnference on Wind Engineering, Porto Alegre, Brazil, pp. 1–11.

Satheeskumar, N., Henderson, D.J., Ginger, J.D., Wang, C.H., 2017b. Three-dimensional finite-element modeling and validation of a timber-framed house to wind loading. J. Struct. Eng. 143 (9) https://doi.org/10.1061/(ASCE)ST.1943-541X.0001850.

Shanmugam, B., Nielson, B.G., Prevatt, D.O., 2009. Statistical and analytical models for roof components in existing light-framed wood structures. Eng. Struct. 31 (11), 2607–2616. https://doi.org/10.1016/j.engstruct.2009.06.009.

Shanmugam, B., Nielson, B.G., Schiff, S.D., 2011. Multi-Axis treatment of typical light-frame wood roof-to-wall metal connectors in design. Eng. Struct. 33 (12), 3125–3135. https://doi.org/10.1016/j.engstruct.2011.07.031.

Sharma, R.N., Richards, P.J., 2005. Net pressures on the roof of a low-rise building with wall openings. J. Wind Eng. Ind. Aerod. 93, 267–291. https://doi.org/10.1016/j.jweia.2005.01.001.

Shao, S., Stathopoulos, T., Yang, Q., Tian, Y., 2018. Wind pressures on 4: 12 -sloped hip roofs of L- and T-shaped low-rise buildings. J. Struct. Eng. 144 (7), 1–20. https://doi.org/10.1061/(ASCE)ST.1943-541X.0002077.

Shao, S., Tian, Y., Yang, Q., Stathopoulos, T., 2019. Wind-induced cladding and structural loads on low-rise buildings with 4:12-sloped hip roofs. J. Wind Eng. Ind. Aerod. 193 (15), 103948 https://doi.org/10.1016/j.jweia.2019.103948.

Sharma, R.N., 2008. Internal and net envelope pressures in a building having quasi-static flexibility and a dominant opening. J. Wind Eng. Ind. Aerod. 96 (6–7), 1074–1083. https://doi.org/10.1016/j.jweia.2007.06.029.

Sharma, R.N., 2012. The Ill-defined parameters of the building internal pressure dynamics problem. In: Proceedings of the 18th Australasian Fluid Mechanics Conference, AFMC 2012 I (December), pp. 1–4.

Sharma, R.N., Richards, P.J., 1997. Computational modelling of the transient response of building internal pressure to a sudden opening. J. Wind Eng. Ind. Aerod. 72 (1–3), 149–161. https://doi.org/10.1016/S0167-6105(97)00244-4.

Sharma, R.N., Richards, P.J., 2003. The influence of Helmholtz resonance on internal pressures in a low-rise building. J. Wind Eng. Ind. Aerod. 91 (6), 807–828. https://doi.org/10.1016/S0167-6105(03)00005-9.

Stathopoulos, T., Luchian, H.D., 1990. Wind pressures on buildings with multi-level roofs. J. Wind Eng. Ind. Aerod. 36 (PART 2), 1299–1308. https://doi.org/10.1016/0167-6105(90)90126-W.

Stathopoulos, T., Saathoff, P., 1991. Wind pressure on roofs of various geometries. J. Wind Eng. Ind. Aerod. 38 (2–3), 273–284. https://doi.org/10.1016/0167-6105(91)90047-Z.

Stathopoulos, T., Mohammadian, A.R., 1986. Wind loads on low buildings with mono-sloped roofs. J. Wind Eng. Ind. Aerod. 23, 81–97.

Stathopoulos, T., Surry, D., Davenport, A.G., 1979. Internal pressure characteristics of low-rise buildings due to wind action. In: 5th International Wind Engineering Conference, vols. 451–63 (Fort Collins, Colorado).

Stathopoulos, T., 2003. Wind loads on low buildings: in the wake of alan davenport's contributions. J. Wind Eng. Ind. Aerod. 91 (12–15), 1565–1585. https://doi.org/10.1016/j.jweia.2003.09.019.

Stathopoulos, T., 1984. Wind loads on low-rise buildings: a review of the state of the art. Eng. Struct. 6 (2), 119–135. https://doi.org/10.1016/0141-0296(84)90005-1.

Stathopoulos, T., Luchian, D.H., 1989. Transient wind induced internal pressures. J. Eng. Mech. 115 (7), 1501–1514.

Stevenson, S.A., El Ansary, A.M., Kopp, G.A., 2019. A practical modelling technique to assess the performance of wood-frame roofs under extreme wind loads. Eng. Struct. 191 (March), 640–648. https://doi.org/10.1016/j.engstruct.2019.04.058.

Surry, D., Lin, J.X., 1995. The effect of surroundings and roof corner geometric modifications on roof pressures on low-rise buildings. J. Wind Eng. Ind. Aerod. 58 (1–2), 113–138. https://doi.org/10.1016/0167-6105(95)00016-K.

Tecle, A.S., Bitsuamlak, G.T., Chowdhury, A.G., 2015. Opening and compartmentalization effects of internal pressure in low-rise buildings with gable and hip roofs. J. Architect. Eng. 21 (1), 1–14. https://doi.org/10.1061/(ASCE)AE.1943-5568.0000101.

Vickery, B.J., 1976. Wind Loads on Low Rise Buildings, Presented at D.R.C. Seminar, Darwin. March 20, 1976, Unpublished, p. 30.

Vickery, B.J., 1986. Gust-factors for internal-pressures in low rise buildings. J. Wind Eng. Ind. Aerod. 23, 259–271.

Vickery, B.J., 1994. Internal pressures and interactions with the building envelope. J. Wind Eng. Ind. Aerod. 53 (1–2), 125–144. https://doi.org/10.1016/0167-6105(94)90022-1.

Vickery, B.J., Bloxham, C., 1992. Internal pressure dynamics with a dominant opening. J. Wind Eng. Ind. Aerod. 41 (1–3), 193–204. https://doi.org/10.1016/0167-6105(92)90409-4.

Walker, G.R., Roy, R.J., 1985. Wind loads on houses in an urban environment. In: Proceedings, 1st Asia Pacific Symposium on Wind Engineering. Roorkee, India, pp. 189–195. Dec.

Wolfe, R.W., LaBissoniere, T., 1991. Structural Performance of Light-Frame Roof Assemblies II . Conventional Truss Assemblies. Report FPL-RP-499. USDA, Forest Products Lab, Madison WI.

Wolfe, R.W., McCarthy, M., 1989. Structural Performance of Light-Frame Roof Assemblies I. Truss Assemblies with High Truss Stiffness Variability. Forrest Products Laboratory[Research Paper: FPL-RP-492].

Wu, C.-H., Kopp, G.A., 2018. A quasi-steady model to account for the effects of upstream turbulence characteristics on pressure fluctuations on a low-rise building. J. Wind Eng. Ind. Aerod. 179, 338–357. https://doi.org/10.1016/j.jweia.2018.06.014.

Xu, Y.L., Reardon, G.F., 1998. Variations of wind pressure on hip roofs with roof pitch. J. Wind Eng. Ind. Aerod. 73 (3), 267–284. https://doi.org/10.1016/S0167-6105(97)00291-2.

Yeatts, B.B., Mehta, K.C., 1993. Field experiments for building aerodynamics. J. Wind Eng. Ind. Aerod. 50 (C), 213–224. https://doi.org/10.1016/0167-6105(93)90076-Z.

Zisis, I., Raji, F., Candelario, J.D., 2017. Large-scale wind tunnel tests of canopies attached to low-rise buildings. J. Architect. Eng. 23 (1), 1–12. https://doi.org/10.1061/(asce)ae.1943-5568.0000235.

Zisis, I., Stathopoulos, T., 2010. Wind-induced pressures on patio covers. J. Struct. Eng. 136 (9), 1172–1181. https://doi.org/10.1061/(asce)st.1943-541x.0000210.